Alma Mater Studiorum – Università di Bologna

DOTTORATO DI RICERCA IN

SCIENZE BIOMEDICHE E NEUROMOTORIE

Ciclo 34

Settore Concorsuale: 06/D6

Settore Scientifico Disciplinare: MED/26

TITOLO TESI

Evaluation of alpha-synuclein RT-QuIC for an early and differential diagnosis of Lewy body disease

Presentata da: Marcello Rossi

Coordinatore Dottorato — Prof.ssa Matilde Yung Follo

Supervisore — Prof. Piero Parchi

Esame finale anno 2021

ABSTRACT

Synucleinopathies are a group of neurodegenerative diseases characterized by tissue deposition of insoluble aggregates of the protein α-synuclein. Currently, the clinical diagnosis of these diseases, including Parkinson's disease (PD), dementia with Lewy bodies (DLB), and multiple system atrophy (MSA), is very challenging, especially at an early disease stage, due to the heterogeneous and often non-specific clinical manifestations. Therefore, identifying specific biomarkers to aid the diagnosis and improve the clinical management of patients with these disorders represents a primary goal in the field.

Real-Time Quaking-Induced Conversion (RT-QuIC) is an ultrasensitive technique originally introduced for prion diseases diagnosis that can detect minute amounts of amyloidogenic proteins in cerebrospinal fluid (CSF) or other biospecimens, taking advantage of their ability to trigger a protein self-aggregation. Recently, the assay was successfully adapted to detect α-synuclein (α-Syn) seeds in biofluid and tissues in patients with synucleinopathies.

Using a wild-type recombinant α-syn as a substrate, we applied the α-Syn RT-QuIC to a large cohort of 953 CSF samples from clinically well-characterized ("clinical" group), or neuropathologically verified ("NP" group) patients with parkinsonism or dementia. Of significance, we also studied patients with prodromal synucleinopathies ("prodromal" group), such as pure autonomic failure (PAF) (*n* = 28), isolated REM sleep behavior disorder (iRBD) (*n* = 18), and mild cognitive impairment due to probable Lewy body (LB) disease (MCI-LB) (*n* = 81).

Our findings show that α-Syn RT-QuIC can accurately detect α-Syn seeding activity across the whole spectrum of LB-related disorders (LBD), exhibiting a mean sensitivity of 95.2% in the "clinical" and "NP" group, while ranging between 89.3% (PAF) and 100% (RBD) in the "prodromal group". Interestingly, only two out of 33 MSA patients displayed seeding activity, highlighting the capability of the assay to discriminate between LBD such as PD and DLB and MSA. Moreover, the observed 95.1% sensitivity and 96.6% specificity in the distinction between MCI-LB patients and cognitively unimpaired controls further demonstrate the solid diagnostic potential of α-Syn RT-QuIC in the early phase of the disease. Finally, 13.3% of MCI-AD patients also had a positive test; of note, 44% of them developed one core or supportive clinical feature of dementia with Lewy bodies (DLB) at follow-up, suggesting an underlying LB co-pathology.

This work demonstrated that α-Syn RT-QuIC is an efficient assay for accurate and early diagnosis of LBD, which should be implemented for clinical management and recruitment for clinical trials in memory clinics.

INDEX

INTRODUCTION 3

α-Synuclein protein 3

α-Syn physiology and pathology 4

Synucleinopathies 6

Parkinson's disease 6

Dementia with Lewy bodies 7

Multiple system atrophy 8

Prion-like features of α-Syn 8

Cellular and tissue spread 9

Heterogeneity across synucleinopathies: α-Syn strains 10

Real-Time Quaking Induced Conversion (RT-QuIC) assay 11

A brief history 11

The need of new early biomarkers for neurodegenerative diseases 13

RT-QuIC assay across synucleinopathies 14

PHD RESEARCH PROJECT 15

AIM OF THE PROJECT 16

MATERIALS AND METHODS 17

Patients and controls for α-Syn RT-QuIC analysis 17

Clinical assessment and diagnostic criteria 19

Neuropathological studies 21

CSF collection and analyses 22

Storage and extraction of plasmid DNA and bacterial transformation 22

Purification of human recombinant α-Syn 23

α-Syn RT-QuIC 24

Statistical analysis 25

RESULTS 27

Setting-up of α-Syn RT-QuIC 27

Purification of recombinant α-Syn 27

Assay reproduction 27

Validation of α-Syn RT-QuIC with neuropathologically assessed cases 29

Diagnostic performance of α-Syn RT-QuIC in the "clinical" group 31

Definition of kinetic parameters and assay reproducibility 32

α-Syn RT-QuIC in patients with parkinsonism 35
α-Syn RT-QuIC in patients with dementia 36
Diagnostic performance of α-Syn RT-QuIC in the "prodromal" group 37
α-Syn RT-QuIC in patients with iRBD and PAF 37
α-Syn RT-QuIC in patients with MCI 38
Comparison of the α-Syn RT-QuIC results across prodromal MCI and probable DLB or AD 39
DISCUSSION AND CONCLUSIONS 41
BIBLIOGRAPHY 46

Evaluation of alpha-synuclein RT-QuIC for an early and differential diagnosis of Lewy body disease

INTRODUCTION

α-Synuclein protein

In the second half of the '80s, a neuron-specific protein of 143 amino acids (aa) was identified for the first time in cholinergic vesicles and nuclear envelope of the *Torpedo californica*, a finding later confirmed also by other groups (1-4). The identification of the bulk of the protein in synaptic vesicles prompted the name *Synuclein*.

In parallel, in pursuing the biochemical characterization of Alzheimer's disease (AD) senile plaques, Ueda and co-workers found two other unknown peptides in addition to Aβ, which were named non- Aβ components (NAC) of AD plaques. The similar concentration of these components in the amyloid fractions suggested a common precursor, later identified in a 140 aa protein: the non- Aβ components precursor (NACP) (5).

Two proteins of 140 aa and 134 aa were purified from the human brain and sequenced one year later. Interestingly, the former showed strong homology with torpedo and rat Synuclein and, especially, a total congruence with NACP. Moreover, a 61% homology was also observed between the two 140 aa and 134 aa proteins, which, for this reason, were renamed α- and β-synuclein, respectively (6). Later, high levels of a third member of the synuclein family, the γ-synuclein, have been detected in ovarian and breast cancer tissues (7).

Nowadays, the α-Synuclein (α-Syn) is probably the most commonly investigated of the three isoforms, given its central role in the pathogenesis of neurodegenerative diseases (8).

α-Syn is a 14 kDa protein encoded by the *SNCA* gene localized on the long arm of chromosome 4 (Chr 4q22.1) (9). It is structurally characterized by three domains: an N-terminal lipid-binding α-helix, an amyloid-binding central domain (NAC), and a C-terminal acid tail (figure 1A). The N-terminal domain (residues 1-60) includes most of the series of 11 aa repeats with highly conserved KTKEGV consensus sequence, a motif also shared with β- and γ-Syn. The positively charged region, analogously to apolipoproteins, forms an amphipathic α-helix able to bind negatively charged lipids (10, 11). The NAC region (residues 61-95), partially located within these repeated sequences, is involved in the oligomerization of the protein due to its hydrophobic composition (11). Finally,

the C-terminal domain (residues 96-140) is characterized by an acidic and glutamate-rich sequence. It presents a random coil structure due to its hydrophobicity and negative charge, making this region involved in different interactions and modifications particularly relevant for physiological and pathological processes (12).

The protein structure appears disordered and characterized by different conformations depending on its soluble or membrane-bound state. In the former case, it is generally found as unstructured protein and, less frequently, as stable tetrameric forms (13-16), whereas, in the membrane-bound state, α-Syn can interact through the N-terminal lipid-binding domain with lipid membranes as artificial liposomes, lipid droplets, and lipid rafts. Despite its capacity to virtually bind all lipid membranes, α-Syn preferentially interacts with membranes with high curvature. Hence the propensity to locate in synaptic vesicles (12, 17, 18).

Likely due to such characteristics, α-Syn is mainly concentrated in the presynaptic terminal and, in contrast to other proteins involved in neurodegeneration, scarcely distributed throughout the neuron (e.g., cell body, dendrites, or axon) (19). This property makes the protein predominantly expressed in the peripheral and central nervous systems, in particular in the neocortex, hippocampus, striatum, thalamus, and cerebellum. However, α-Syn is not limited to nervous tissues and CSF, and is also found in red blood cells, blood plasma, platelets, lymphocytes, blood vessels, testis, heart, lung, liver, kidney, and muscle (12, 20).

α-Syn physiology and pathology

According to the soluble or membrane-bound state and cellular localization, α-Syn contributes to several functions, including suppression of apoptosis in dopaminergic neurons (21), glucose homeostasis (22, 23), calmodulin activity modulation (24), molecular chaperone, and SNARE complex assembly (25, 26), maintenance of polyunsaturated fatty acids levels (27), prevention of unsaturated lipids oxidation in vesicles (28), promotion of neuronal differentiation by Ras activation (29), modulation of dopamine biosynthesis (30) and regulation of vesicle trafficking (31).

α-Syn is subjected to multiple posttranslational modifications, which can determine changes in protein structure and charge, leading to alteration in binding affinity with other molecules and overall protein hydrophobicity. Accordingly, although the phenomenon is still largely unexplored in the physiological context, it has become clear that such modifications may convert ordinary functions into pathological activities. Hence, different post-translational modifications, including serine and tyrosine phosphorylation, ubiquitination, nitration, glycation, glycosylation, and C-

terminal truncation, have been extensively investigated to elucidate their effect in modulating α-Syn aggregation and toxicity rather than their role on the functional and physiological properties of the protein (12, 32).

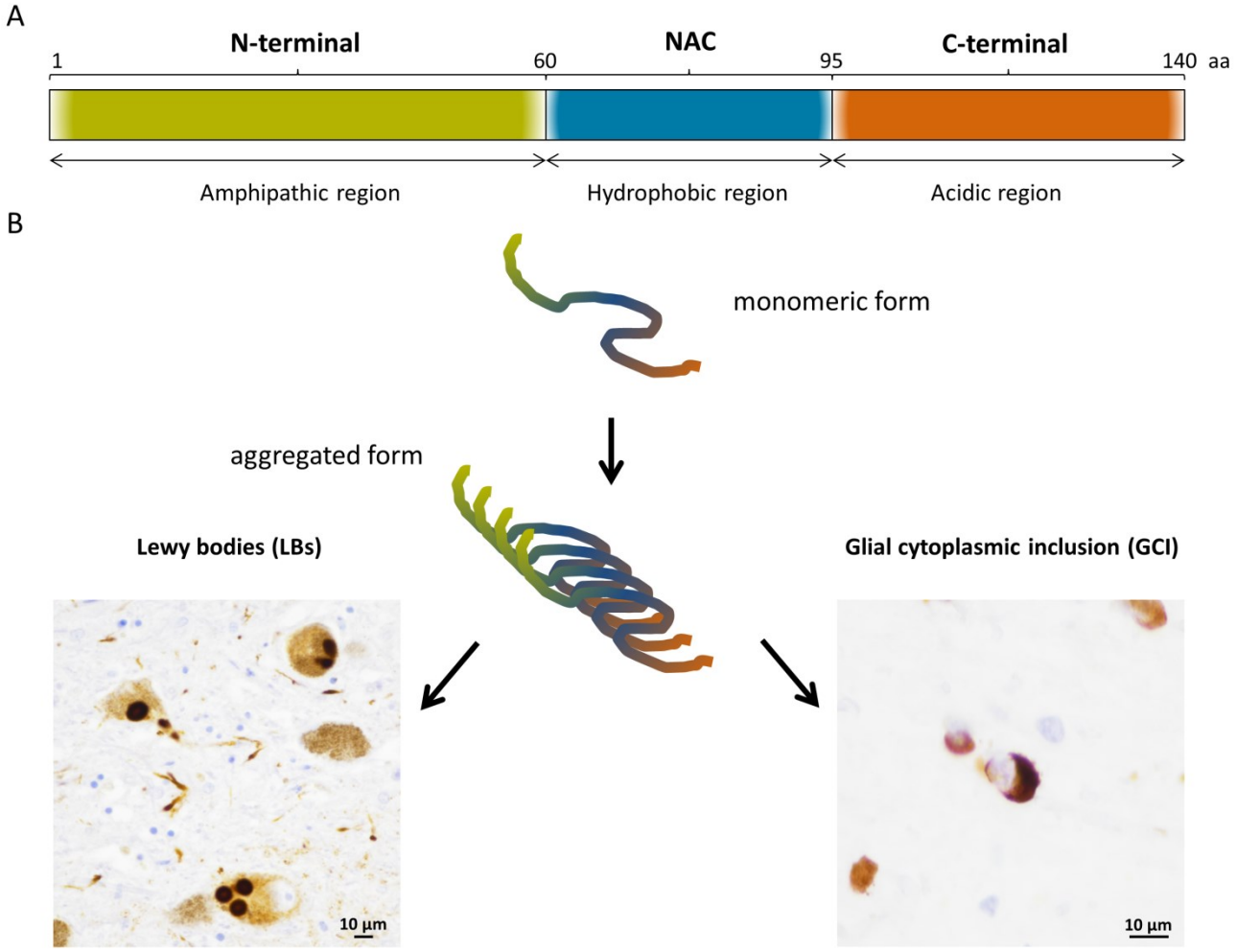

Figure 1. Schematic representation of primary structure and pathological aggregation of α-Syn protein. A) Primary structure of α-Syn protein characteristic domains: amphipathic, hydrophobic and acidic regions. B) Images of disease-specific lesions (LB and GCI) caused by pathological aggregation of α-Syn. Immunostaining was carried out with LB509 antibody (dilution 1:100, Thermo Fisher) and captured at 40X and 60X magnification

With the identification of α-Syn as the main actor in Parkinson's disease (PD) pathology (8, 33), the protein became the focus of intense investigation and was later identified as the pathological hallmark of other neurodegenerative diseases, including dementia with Lewy bodies (DLB) and multiple system atrophy (MSA). Because of the intriguing common characteristic, this novel group of neurodegenerative diseases was referred to as "synucleinopathies."

Synucleinopathies

In 1997 Polymeropoulos and colleagues identified, for the first time, the A53T mutation in *SNCA*, the α-Syn gene, in the Contursi kindred and three smaller Greek families affected by inherited PD. In the same year, Spillantini et al. reported a strong immunoreactivity for α-Syn in Lewy bodies (LBs), the hallmark of both PD and DLB pathology (8, 33). LBs have been initially described in dopaminergic neurons of the substantia nigra as spherical cytoplasmic eosinophilic inclusions surrounded by a halo, but their precise protein composition was hitherto unknown. The same authors also found that antibodies raised against amino-terminal and carboxyl-terminal sequences of α-Syn protein strongly stain Lewy neurites (LNs) (33). These are abnormal neurites containing filaments similar to those found in LBs that also represent a common pathological feature of PD and DLB (34, 35). Cytoplasmic inclusions containing α-Syn are also the major histological hallmark of MSA, although they are typically placed in oligodendrocytes rather than neurons and, for this reason, named glial cytoplasmic inclusions (GCIs) (Figure 1B). Although such diseases share the proteinaceous origin of the pathological cellular deposits, they differ for anatomical areas involved and clinical features (19).

Parkinson's disease

Parkinson's disease, described for the first time by James Parkinson in 1819, represents the most common synucleinopathy and neurodegenerative movement disorder worldwide. It affects almost 200.000 people in Italy and shows an incidence rate that is strongly age-dependent (36, 37). Cardinal motor manifestations include bradykinesia, rigidity, and rest tremor (38). Other features include postural instability and several nonmotor symptoms such as cognitive decline, anxiety, depression, sleep disturbance, and dysautonomia. The latter is virtually present in all patients affected by PD and includes constipation, a symptom also observed in the very early disease stage (39, 40). Similarly, anosmia may precede the clinical manifestation of the disease for many years and occurs in as many as 90% of PD patients (41). Early non-PD specific symptoms may also be observed in prodromal syndromes of the disease that may evolve to PD or DLB, such as pure autonomic failure (PAF), a rare synucleinopathy affecting the autonomic nervous system and clinically characterized by orthostatic hypotension, and idiopathic rapid eye movement (REM)

sleep behavior disorder (RBD), characterized by abnormal movements in the absence of muscle hypotonia during the REM sleep (42, 43).

The development of dementia characterizes a large percentage of the PD population. Evidence indicates that PD patients have a fourfold chance to develop cognitive problems, with 50% and 83% of the subjects that evolve dementia within 10 and 20 years after disease onset, respectively (44-46). When dementia syndrome occurs more than one year from PD onset, the eponym PD Dementia (PDD) is assigned. The occurrence of cognitive decline best reflects the progression of the brain pathology, where α-Syn aggregates spread from the brainstem structures, in the early stage of disease, to neocortical regions in the latter stages. In this area, the α-Syn pathology presents much more severe lesions (up to 10-fold higher) in PDD than in PD (47).

Dementia with Lewy bodies

DLB represents the second most common synucleinopathy and accounts for 7.5% of all cases of dementia in clinically-based studies. However, the data is probably underestimated since neuropathological studies assessed a disease prevalence among neurodegenerative dementias of 16-24% (48, 49).

PDD shares many clinical features with DLB. The diagnostic criterion to differentiate the two disease subtypes, assigned by clinical neurologists, only consider the time of dementia appearance after the initial manifestation of motor symptoms: while patients that manifest dementia after one year from the onset of motor symptoms are classified as PDD, subjects that develop dementia before or within one year from the diagnosis of PD are diagnosed as DLB.

Before the full development of DLB, the manifestation of one or more of the core clinical features characteristic of the disease could occur, and, in this case, is usually accompanied by mild cognitive complaints (50). Hence, the prodromal phases, referred to as pre-dementia stages with signs or symptoms indicating the following development of DLB, may consist of motor symptoms and signs, sleep disorders, autonomic dysfunction, neuropsychiatric disturbance, but also to be relative to cognitive deficits (51). Pursuing such evidence, McKeith and coworkers recently proposed diagnostic criteria for mild cognitive impairment (MCI) with Lewy bodies (MCI-LB), in the attempt to better define early prodromal cognitive syndromes with strong propensity to evolve in DLB (52).

Multiple system atrophy

Multiple system atrophy (MSA) is a rapidly progressive neurodegenerative disease affecting approximately 0.6-0.7 cases per 100,000 people annually (53). Nowadays, MSA includes three historically separated conditions named olivopontocerebellar atrophy, striatonigral degeneration, and Shy-Drager syndrome. In 2007, two subtypes were officially defined based on their clinical phenotypes: MSA-P, which encompasses patients with parkinsonism as the predominant feature, and MSA-C, which denotes prominent cerebellar symptoms (54).

MSA manifests a more rapid progression than PD (6-9 years for MSA and about 12 years for PD). However, as for PD, a neuropathological investigation is necessary to reach a definite diagnosis (55, 56). Similar to PD, PDD and DLB, unspecific symptoms and signs may occur several months or years before the onset of the full-blown disease manifestation. Sleep disorders, autonomic failure, and respiratory alterations are well-known symptoms of established MSA. When presenting early and preceding ataxia or parkinsonism, they should raise the suspicion of MSA (57). However, MSA manifests distinct neuropathologic features compared to LB disorders such as PD and DLB. Indeed, the α-Syn aggregates, present in oligodendrocytes as GCIs, are mainly distributed in three functional systems: the olivopontocerebellar system, the striatonigral systems, and the autonomic system (58). Although α-Syn neuronal inclusions (NIs) are scarcely represented, a subgroup of subjects with long disease course and severe temporal atrophy may show abundant NIs in the limbic structures (59).

Prion-like features of α-Syn

The term prion derives from “proteinaceous” and “infectious” and specifically describes the unique properties of the etiologic agent of a heterogeneous and rare group of neurodegenerative diseases, called prion diseases. In these disorders, the cellular prion protein (PrP^{C}), physiologically expressed in the nervous system, is converted into its pathological counterpart (PrP^{Sc}, from “Scrapie,” a prion disease that affects ovines) through a post-translational process during which it acquires a high beta-sheet content. Evidence strongly argues that PrP^{Sc} induces a structural conversion of PrP^{C} acting as a template, triggering a progressive aggregation of the new misfolded protein. This mechanism confers to the prion the ability to spread between organisms and tissues, with infectious properties. Despite the lack of differences in the primary structure, PrP^{Sc} can

generate different strains, encoding structural information, and biochemical and infectious properties. Hence, the characteristic heterogeneity of prion diseases (60, 61).
Several studies on α-Syn biochemical features, aggregation, and spreading processes have suggested strong similarities between PrP and α-Syn in recent years.

Cellular and tissue spread

The demonstration that distinct brain regions are progressively involved by α-Syn pathology depending on the disease stage represented key evidence supporting the prion-like properties of α-Syn. Neuropathological studies suggested a systematic progression of LN and LB lesions during disease evolution, from the involvement of the dorsal motor nucleus and, frequently, in the most mildly affected cases, the anterior olfactory nucleus, to the involvement of the neocortex in the most severe cases (62). The idea of a prion-like spreading mechanism was further reinforced by observing Lewy pathology in fetal human midbrain neurons, therapeutically implanted into the striatum of patients with advanced PD, ten or more years after transplantation (63, 64). Such evidence prompted further experimental grafting studies to explore better how this apparent spread may occur (65, 66). The acceleration of synucleinopathy in young α-Syn transgenic mice after the injection of brain homogenates from sick transgenic animals further supported the prion-like properties of α-Syn (67). Finally, the prion-like spreading ability of misfolded α-Syn protein was also reproduced with synthetic aggregates inoculated in animals or cellular models (68-71).
Although the α-Syn cell-to-cell spreading mechanism is not fully understood, it has been shown that small amounts of α-Syn can undergo secretion through a vesicular mechanism and, in particular through exosomes, the luminal membranes of multivesicular bodies (mvbs) that are typically targeted for degradation into lysosomes (72, 73).
It is also possible that oligomeric forms of α-Syn become particularly susceptible to release. Jang et al. showed that vesicles do not only preferentially secrete the misfolded α-Syn but also increases the process of release, suggesting a clearance mechanism of damaged proteins (74). Moreover, transmembrane or extracellular receptors seem then involved in the internalization of misfolded/aggregated α-Syn, advancing the hypothesis of the roles of other proteins in the α-Syn uptake (75-77).
Most findings relative to α-Syn cellular spread were obtained in neuronal cells, and, for this reason, the hypothesis of a neuronal origin of α-Syn aggregates in MSA is considered, despite the

predominant oligodendroglial GCIs. Indeed, while a basal expression of α-Syn has been recently demonstrated in oligodendrocytes and might represent a potential trigger of protein accumulation, the uptake of the protein from neurons or the extracellular environment may also be considered a possible trigger of protein accumulation. The latter mechanism is supported by evidence indicating a transfer of α-Syn from neuron-to-neuron or neuron-to-oligodendrocyte (65, 78, 79).

The demonstration by Braak and colleagues of the involvement of dorsal motor and anterior olfactory nucleus in the first stage of PD raised the hypothesis that PD pathology might originate in synapses of the peripheral nervous system (PNS) and successively spread in the central nervous system. In particular, the enteric tract represented the center of the hypothesis (80). The concept was further supported by finding pathological α-Syn aggregates in the PNS of PD patients up to 20 years before diagnosis (81-83). Other studies showed that α-Syn fibrils transmitted by oral, intraperitoneal, intramuscular, and intravenous inoculation led to widespread α-Syn pathology in the CNS of transgenic mice (84, 85). The observed pattern reported strong similarities with the spreading model documented in prion disorders, including bovine spongiform encephalopathy and scrapie (86-88).

All this evidence supports the idea that prion-like mechanism is not only related to prion diseases but also characterizes α-Syn pathology and, probably, other neurodegenerative diseases related proteins.

Heterogeneity across synucleinopathies: α-Syn strains

Although misfolded β-sheet rich forms of α-Syn characterize all the spectrum of α-synucleinopathies, the pathological form of the protein is also found in a significant proportion of individuals affected by Alzheimer's disease, in several other rare disorders, and, as incidental Lewy body disease in about 10% of elderly individuals lacking neurological symptoms (55). The phenotypic heterogeneity observed in α-Synucleinopathies shows strong similarities with prion diseases (55, 61, 89).

In microbiology, strains are classically defined by differences in their genetically coded information which, in turn, determine well-defined pathogenic patterns and clinical symptoms. In the absence of a genetic code, the vast and reproducible heterogeneity observed in prion diseases has been explained as a consequence of specific misfolding of the PrP^{Sc} (90). Analogously, evidence

suggested that recombinant α-Syn monomers may form synthetic α-Syn aggregates with distinct conformations and biological activities (91-95). Bossuet and coworkers showed that, under physiological salt concentrations, α-Syn monomers could generate aggregates with a cylindrical shape, named fibrils, and with a flat structure, called ribbons. Biophysical and biochemical analysis confirmed such structural differences and, intriguingly, following studies reported divergent biological activities, such as cytotoxicity and ability to induce α-Syn pathology in vivo (92, 93).

Strain properties were also investigated and confirmed from α-Syn aggregates isolated from human brains. Prusiner's group found that pathological α-Syn extracted from MSA patients, but not those from PD, PDD, and DLB patients, could propagate in α-Syn140*A53T–YFP mice (96). With a similar cellular assay, Yamasaki and colleagues demonstrated the presence of different inclusions in cells infected by PD and MSA α-Syn aggregates (97). Such strain features were further confirmed by inoculation of preformed fibrils (PFF) or brain homogenates in animal models (95, 96, 98). Moreover, Peng et al., other than describing a more potent seeding capacity of MSA (GCI-α-Syn) aggregates than PD (LB-α-Syn) ones, in line with the findings reported above, demonstrated the role of oligodendrocyte environment in the generation of GCI-α-Syn strain (99).

Finally, if biochemical and biological data strongly suggest the existence of α-Syn strains, the recent structural findings overwhelmingly support this hypothesis. Through fluorescent probes, NMR spectroscopy, and electron paramagnetic resonance, differences in the conformational properties of PD and MSA α-Syn extracts were confirmed (100). Moreover, cryo-electron microscopy studies support the findings highlighting structural divergences between MSA and DLB filaments (101).

Real-Time Quaking Induced Conversion (RT-QuIC) assay

A brief history

When the "protein-only mechanism" was theorized for the first time in the attempt to describe the propagation of the PrP as the sole pathogenic agent of transmissible spongiform encephalopathies, different studies tried to better define and reproduce the mechanism *in vitro* (60, 102). Hence, in the mid-'90s, Kocisko and colleagues successfully generated aggregated species of PrP in a cell-free assay. In this study, the ability of PrP^{Sc} to enroll and convert its physiological counterpart was confirmed by incubating an excess of PrP^{Sc} isolated from prion-

infected hamsters with a 35S-labelled recombinant hamster PrP^C. The observation of proteinase K (PK)-resistant labeled PrP demonstrated the capability of the pathological protein to structurally convert the PK-sensitive form in misfolded species (103). Later, a considerable implementation of the *in vitro* conversion assay was obtained by introducing cyclical sonication and incubation steps, which speeded up the PrP^C conversion through fibrils breakage and generation of new nucleation sites for monomers aggregation during the incubation phases. The assay was named protein misfolding cyclic amplification (PMCA) (104). However, the infectious nature (105) of the final misfolded PrP^{Sc} product, the sensitivity to contaminants, and the time-consuming protocol led to new technical improvements. The replacement of brain homogenate with recombinant PrP as reaction substrate and the swap of sonication with automated shaking (106, 107) contribute to a solid implementation of the in vitro PrP^{Sc} amplification methodology. Finally, taking advantage of the introduction of the Thioflavin T (ThT) to detect the polymerization of rec-PrP into amyloid (106, 108), Caughey's lab developed the first version of the Real-Time Quaking Induced Conversion (RT-QuIC), where the progressive amplification of misfolded PrP was monitored in real-time by the fluorescence emission of ThT (109) (Figure 2).

The capacity to unprecedentedly detect minute amounts of PrPSc was successively confirmed in the application of the assay to cerebrospinal fluid (CSF) and other non-nervous tissues of animals and humans affected by prion diseases (110-113).

Nowadays, RT-QuIC is part of the diagnostic criteria for sporadic CJD (sCJD). Efforts are ongoing to expand the RT-QuIC application to the early diagnosis of prion-like neurodegenerative disorders.

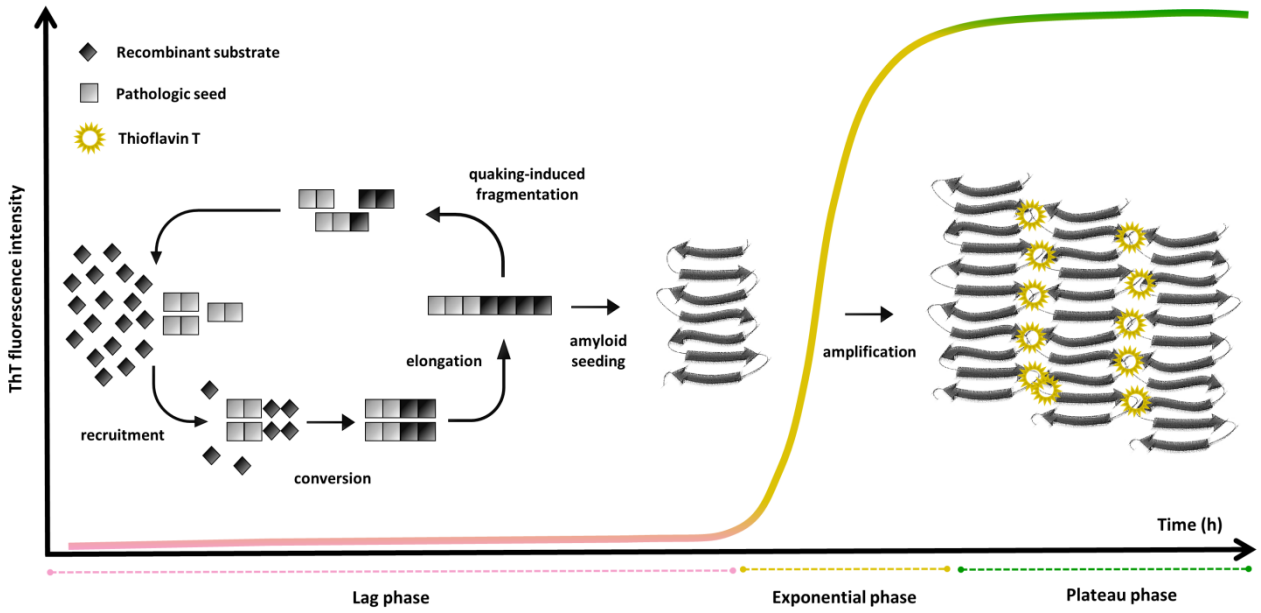

Figure 2. Schematic representation of the RT-QuIC reaction. The RT-QuIC reaction phases may be summarised in lag phase, exponential phase and plateau phase. During the former step, seeds structurally convert the protein recombinant substrate triggering a protein aggregation. With the formation of the first fibrils the system detects the fluorescent signal of ThT, a dye with a strong affinity with the fibrillar protein state (exponential phase). Eventually, when all the substrate is incorporated into fibrils, a plateau phase is observed. The figure was adapted from Candelise et al., Acta Neuropath Commun 2020 (114).

The need of new early biomarkers for neurodegenerative diseases

As described above, whereas initially the "protein-only mechanism" was theorized on prion protein studies, the capacity of misfolded proteins to induce further self-propagation is now a broadly recognized feature of the proteins underlying neurodegenerative diseases. Several findings suggest that the aggregation process, based on the structural conversion of a normally folded protein through a pathological template, is shared among the most known proteins associated with neurodegeneration, including β-amyloid, tau, α-synuclein, and TDP-43. Hence, "protein seeds" are defined as misfolded proteins able to trigger self-propagation and the formation of protein aggregates (115).

The overlapping symptoms and the presence of toxic oligomers years before the clinical manifestation make the RT-QuIC a valuable and robust assay for more selective discrimination of diseases and a potential capability of early diagnosis. Indeed, current diagnostic criteria usually require the combination of multiple diagnostic investigations, clinical findings, and an adequate follow-up of several years to reach the accurate identification of the disorder (114). Moreover, imaging, neuropsychological and neurophysiological examinations are often only supportive of the clinical findings. Similarly, except for AD, where specific tau and β-amyloid protein isoforms levels concord with the amount of proteins deposition in the brain, current CSF biomarkers such as total tau, 14-3-3, and neurofilament proteins only reflect the neuronal damage and, for this reason, do not describe a specific pathology but support the clinical picture (116).

Therefore, in neurodegenerative diseases, where post-mortem neuropathologic examinations remain the gold standard for a definite diagnosis, the success of prion RT-QuIC strongly suggested further developments of the assay and the application to the whole spectrum of the neurodegenerative disorders. Among this large family, with a growing number of published studies in recent years, the new and more promising application of RT-QuIC seems to be associated with synucleinopathies.

RT-QuIC assay across synucleinopathies

Synucleinopathies are widely heterogeneous in clinical manifestation, response to therapy, and rate of progression. Moreover, they may initially manifest as prodromal syndromes, such as PAF, RBD, which often evolve in PD, PDD, DLB or MSA (42, 43). Analogously, they can be associated at the onset with mild cognitive impairment (MCI) which, following the strategies implemented for AD, has been recently recognized as a prodromal clinical entity (i.e., MCI-LB) belonging to the DLB clinical spectrum (48, 52, 117, 118). The difficulties of an early diagnosis due to the heterogeneous range of clinical manifestation is further complicated by overlapping symptoms with atypical parkinsonisms such as progressive supranuclear palsy (PSP) and corticobasal degeneration (CBD), two primary tauopathies, and other neurodegenerative dementias such as AD or frontotemporal dementia (FTD). For this reason, the clinicopathological rate of accordance in autopsy verified cohorts remain partially inaccurate (i.e., 92.6% for PD, 81.6% for DLB, 62–78.8% for MSA) (119-122).

Fairfoul and colleagues applied for the first time the RT-QuIC to CSF of 20 clinically diagnosed PD and 12 neuropathologically confirmed DLB cases. The new α-Syn RT-QuIC showed a 100% specificity and 92-95% sensitivity (123). Subsequently, Soto's group obtained similar results through the adaptation of the previously reported prion PMCA assay. Their study discriminated PD patients from those affected by other neurologic or neurodegenerative disorders with a sensitivity of 88% and a specificity of 97% (124). Evidence recommending the application of α-Syn RT-QuIC to the clinical diagnosis and strain discriminations of synucleinopathies were progressively confirmed by other studies (125-132). Intriguingly, the assay also showed an optimal performance when applied to skin samples and in prodromal synucleinopathies such as RBD, PAF and MCI (130, 131, 133, 134).

Despite the enormous success, the α-Syn RT-QuIC protocols still differ among the laboratories, with several assay variables remaining to explore. In particular, although all the elements that contribute to the reaction mix are crucial, as observed for the prion RT-QuIC (135, 136), the substrate remains the main factor able to influence the assay performance.

PHD RESEARCH PROJECT

The laboratory of Neuropathology at ISNB (Bologna, Italy) is currently a worldwide leader in the field of prion diseases and the application of prion RT-QuIC. The implementation of the prion aggregation assay was successful also thanks to a fruitful collaboration with the Caughey's lab (NIAID, NIH, Montana, USA). With the purpose to improve and adapt the RT-QuIC to the study and diagnosis of synucleinopathies, this project aimed to faithfully reproduce in our lab the α-Syn protocol elaborated by Groveman and colleagues (127) followed by its validation in the whole spectrum of synucleinopathies. The results of the study are for the most part published in two recent publications that investigated with α-Syn RT-QuIC the larger cohort of synucleinopathies so far analyzed and, for the first time, prodromal MCI-LB patients:

- Rossi M et al., Ultrasensitive RT-QuIC assay with high sensitivity and specificity for Lewy body-associated synucleinopathies. Acta Neuropathol. 2020 Jul;140(1):49-62. doi: 10.1007/s00401-020-02160-8 (130).

- Rossi M et al., Diagnostic Value of the CSF α-Synuclein Real-Time Quaking-Induced Conversion Assay at the Prodromal MCI Stage of Dementia With Lewy Bodies. Neurology. 2021 Jul 1:10.1212/WNL.0000000000012438. doi: 10.1212/WNL.0000000000012438 (131)

AIM OF THE PROJECT

1. **Setting-up of α-Syn RT-QuIC**
    a. *Purification of recombinant α-Syn*
    b. *Assay reproduction*
2. **Validation of α-Syn RT-QuIC with neuropathologically assessed cases**
3. **Diagnostic performance of α-Syn RT-QuIC in the "clinical" group**
    a. *Definition of kinetic parameters and assay reproducibility*
    b. *α-Syn RT-QuIC in patients with parkinsonisms*
    c. *α-Syn RT-QuIC in patients with dementia*
4. **Diagnostic performance of α-Syn RT-QuIC in the "prodromal" group**
    a. *α-Syn RT-QuIC in patients with iRBD and PAF*
    b. *α-Syn RT-QuIC in patients with MCI*
5. **Comparison of the α-Syn RT-QuIC results across prodromal MCI and probable DLB or AD**

MATERIALS AND METHODS

The study was conducted according to the revised Declaration of Helsinki and Good Clinical Practice guidelines. Informed consent was given by study participants or the next of kin.

Patients and controls for α-Syn RT-QuIC analysis

A total of 827 CSF samples referred to the Laboratory of Neuropathology, Institute of Neurological Sciences of Bologna (ISNB), Italy between 2005 and 2020 and 126 samples referred to the Alzheimer Center Amsterdam, VU Medical Center (VUmc) Amsterdam, the Netherlands, between 2003 and 2020, were analyzed. The cohort included 142 patients with a post-mortem CNS neuropathological assessment (i.e., "neuropathological" [NP] cases) and 811 patients with a clinical diagnosis reached after a comprehensive evaluation and a significant follow-up (table 1).

The NP group comprised patients with progressive dementia, more often with a rapidly progressive course, or atypical parkinsonism evaluated at ISNB, including the following diagnostic categories: DLB, AD, CJD, FTLD, MSA, PSP, Encephalitis, Vascular dementia, and other dementias. Based on the protein aggregates assessment by immunochemistry, the group was further divided into LB α-Syn + and LB α-Syn - subgroups (see below for further details).

The "clinical" group included 270 patients from ISNB, 62 cases lacking symptoms and signs suggesting an underlying progressive neurodegenerative disorder (i.e., chronic headache and narcolepsy type 1 with or without associated RBD) and 208 patients fulfilling the current diagnostic criteria of probable or clinically established disease for one of the following disorders/syndromes: PD (38), MSA (54), PSP (137), CBS (138), DLB (139), and AD (140).

The "prodromal" group encompassed 335 patients showing clinical manifestation of prodromal synucleinopathies such as isolated RBD (iRBD) (141), PAF (142, 143), and MCI (144) from ISNB (all groups) and VUmc (only MCI). Among them, 58 individuals lacking objective neurological signs and cognitive decline were also included as controls.

Whereas the ISNB cohort comprised consecutive patients with MCI, the VUmc cohort included patients selected from the Amsterdam Dementia Cohort (145) and included MCI-LB patients, age-matched, biomarker-confirmed MCI-AD patients, and SCD patients. In both cohorts, MCI was diagnosed according to current diagnostic criteria (144).

Patients with evidence of non-neurodegenerative causes of cognitive decline, including severe white matter lesions on neuroimaging (Fazekas score=3) (146) were excluded.

Finally, to explore potential differences in the α-Syn RT-QuIC across the disease course in prodromal MCI and the clinically diagnosed phase, we incremented the investigated AD group with the analysis of further 206 probable AD (140) patients CSF .

Table 1. Study cohort and demographic findings.

Diagnostic category	n	Female (%)	Age at LP (yrs)	Time between clinical onset and LP (mos)	Follow-up duration (mos)^	Time between clinical onset and last visit (yrs)
Definite NP cohort						
LB- α-Syn +	21	9 (42.9)	75.8±6.3	12.2±28.9	3.9±8.8	2.2±2.5
● DLB	14	6 (42.8)	76.9±5.4	17.3±34.1	5.0±10.4	1.7±2.9
● Dementia with incidental LB	7	3 (42.9)	74.3±7.7	2.0±1.8	1.1±1.1	0.3±0.2
LB- α-Syn –	121	54 (44.6)	68.0±10.2	3.8±12.9	5.2±13.8	0.7±1.7
● AD	18	9 (50.0)	76.4±7.5	1.6±2.5	1.9±2.6	0.3±0.3
● PSP	1	0 (0)	64	108	30	11.5
● MSA	2	1 (50.0)	62.5±7.8	40.5±54.4	68.5±28.9	9.1±2.1
● Syn-controls*	100	41 (41.0)	66.7±10.0	2.1±3.3	4.1±11.1	0.5±0.7
Clinical cohort						
DLB	34	9 (26.5)	73.2±7.5	78.8±105.8	14.9±21.4	7.8±8.7
AD	43	22 (52.2)	66.3±7.8	43.4±39.7	12.7±15.8	4.7±3.5
PSP/CBS	30	19 (63.3)	70.7±6.7	47.0±32.9	8.9±15.0	4.7±2.8
MSA	31	12 (38.7)	60.7±8.6	55.2±42.0	23.4±16.3	6.4±3.6
PD[#]	70	19 (27.1)	62.2±8.8	56.8±45.8	31.6±35.9	7.4±4.2
Clinical controls	62	30 (48.4)	53.9±15.4	158.7±152.5	30.2±27.5	15.5±13.5
Prodromal cohort						
PAF	28	11 (39.3)	65.5±8.5	119.3±62.5	43.9±50.4	13.6±6.9
iRBD	18	6 (33.3)	68.2±7.7	71.5±60.7	10.6±15.1	6.9±4.7
MCI-LB	81	11 (13.6)	70.7±6.6	50.8±71.6	28.4±28.9	6.5±6.3
● ISNB	45	10 (22.2)	72.8±5.8	54.9±88.1	20.1±23.6	6.3±7.3
● VUmc	36	1 (2.8)	67.7±6.5	44.3±33.0	42.2±32.0	6.9±4.1
MCI-AD	120	55 (45.8)	68.6±7.4	34.6±28.6	33.4±27.9	5.7±3.3
● ISNB	58	29 (50.0)	70.6±8.6	39.1±33.0	16.9±22.0	4.7±3.8
● VUmc	62	26 (41.9)	66.7±5.3	30.2±22.9	50.4±22.7	6.7±2.4
Unsp-MCI	30	9 (30.0)	65.4±9.3	30.3±20.3	10.9±11.3	3.5±1.6
SCD/CTRL	58	12 (20.7)	67.2±4.3	97.9±121.9	27.8±27.9	10.9±10.9
● ISNB	30	11(3.7)	67.2±5.7	136.7±148.7	27.7±31.3	13.3±12.7
● VUmc	28	1(3.6)	67.3±1.5	76.3±35.1[°]	21.6±20.8	6.4±2.9
Probable AD cohort	206	124 (60.2)	68.8±9.4	32.4±27.6	8.0±16.6	3.1±2.8

[^]The follow-up duration was calculated from LP to the last visit (or death). *Includes neuropathological cases diagnosed as Creutzfeldt-Jakob disease (n=66), malignancy (n=3), vascular disease (n=8), encephalitis

(n=11), Wernicke encephalopathy (n=3), frontotemporal lobar degeneration plus amyotrophic lateral sclerosis (n=1), non-specified tauopathy (n=1), dementia lacking distinctive pathology (n=6), autosomal dominant cerebellar ataxia (n=1). # Includes 52 clinically established and 18 probable cases. °The onset was calculated from the appearance of cognitive complaints. List of abbreviations: LP, lumbar puncture; DLB, dementia with Lewy bodies; AD, Alzheimer's disease, PD, Parkinson's disease; PSP, progressive supranuclear palsy; CBS, corticobasal syndrome; MSA, multiple system atrophy; PAF, pure autonomic failure; iRBD, isolated REM sleep behaviour disorder; MCI, mild cognitive impairment; α-Syn, α-Synuclein.

Clinical assessment and diagnostic criteria

The clinical history and the results of neurological examination/s and diagnostic investigations were collected for each patient. Moreover, the brain magnetic resonance imaging (MRI, n= 534), cerebral 129I-ioflupane SPECT (DaTSCAN) (n=193), cardiac 123I-metaiodobenzylguanidin (MIBG)-SPECT (n=94) and all-night polysomnography (PSG, n=172) were obtained when available. For AD, DLB and MCI groups, results of neuropsychological examination(s), data of Mini-Mental State Examination (MMSE), and CSF values of AD core biomarkers (table 2) were also obtained. All patients with suspected autonomic failure (AF) (n=158) were assessed by a battery of cardiovascular reflex tests, including head-up tilt test (10 min at 65°), Valsalva maneuver (40 mm Hg for 15 sec), deep breathing (6 breaths/min), and sustained handgrip (one-third of maximal effort for 5 min). Patients with the diagnosis of narcolepsy type 1 (n=15) underwent the multiple sleep latency test, polygraphic assessment of cataplexy, and the evaluation of CSF orexin levels. After CSF collection, most patients belonging to the "clinical" group were longitudinally followed-up at the ISNB [i.e., the follow-up duration was > 2 years in 99 (36.5%), and > 1 year in 142 cases (52.3%)]. In the "prodromal" group, the VUmc patients were annually followed up with clinical evaluation (history and neurological examination) including neuropsychological testing, whereas the follow-up data relative to ISNB patients was obtained by outpatient neurological visits at the Center for Cognitive Disorders. Overall, a longitudinal follow-up was carried out in the 72.6% of "prodromal" patients [(the follow-up duration was > 2 years in 133 (44.0%), and > 1 year in 175 cases (58.1%)].

The "clinical" group included only patients with a "probable" or "clinically established" (for PD only) diagnosis at last follow-up of PD, MSA, PSP, CBS, DLB, and AD, according to international criteria. Among them, ten patients with the clinical diagnosis of PD (n=8) or DLB (n=2) carried single allele mutations known to be associated with LBD in the glucocerebrosidase gene (GBA)

(N370S, L444P, R131C, E326K, n=9) or in the Leucine Rich Repeat Kinase 2 gene (LRRK2) (G2019S, n=1) were included. The cases fulfilling the criteria for more than one probable disease (e.g., concurrent probable diagnosis of PSP and MSA) were excluded.

In the "prodromal" group, the term iRBD was used to refer to RBD occurring in the absence of any associated neurological sign or other possible cause (42). Only patients with PAF presenting with autonomic failure (AF) as the sole clinical manifestation for at least five years were considered (147). iRBD and PAF subjects that were clinically phenoconverted at last follow-up (e.g. DLB, PD, and MSA) were evaluated separately.

Based on the clinical features, AD core markers, imaging, neurophysiological data, and evolution at the last follow-up MCI patients were classified in four groups: 1) MCI-LB, 2) MCI-AD, 3) MCI due to other neurodegenerative disorders (unsp-MCI), and 4) controls. The presence or absence of clinical core features of DLB was determined according to the definitions and guidelines provided by the DLB Consortium (52, 139). PD-MCI patients were excluded from the studied cohort through the application of the one-year rule. The MCI-LB group included 81 individuals (ISNB, n=45; VUmc, n=36) who fulfilled the current criteria for probable MCI-LB (52) at lumbar puncture (LP, n=77) or during follow-up (n=4, two from VUmc, two from ISNB). Among them, three had possible MCI-LB and one unsp-MCI at baseline (at LP).

The MCI-AD group consist of 120 patients (ISNB, n=58; VUmc, n=62) who lacked clinical evidence of DLB core features at the time of LP, and revealed in vivo evidence of AD pathology as defined by abnormally reduced amyloid-beta 1-42:amyloid-beta 1-40 (Aβ42:Aβ40) ratio (ISNB) or decreased Aβ42 levels (VUmc), combined with increased total (t)-tau and phospho (p)-tau concentrations (A+,T+,N+) in CSF or an abnormal p-tau:Aβ42 or t-tau:Aβ42 ratio (140, 148, 149).

Thirty patients were grouped in "unspecified" MCI (Unsp-MCI) since they did not embrace the inclusion criteria for MCI-LB (absence of core clinical features and biomarker evidence of DLB at LP and during follow-up) and lacked in vivo evidence of AD pathology by CSF analysis.

Among the 58 "control" patients for the prodromal cohort, 30 individuals (from ISNB) were clinically diagnosed as chronic headache or narcolepsy type 1 and no clinical evidence of an underlying progressive neurodegenerative disorder, and 28 individuals (from VUmc) reported subjective experience of cognitive decline but had normal baseline cognition, defined by results of cognitive assessment within normal ranges. Furthermore, they had at least one follow-up assessment (>8 months from baseline) with an unchanged diagnosis (150).

None of the patients in the "clinical" and "prodromal" groups underwent a post-mortem neuropathological examination.

Table 1. Result of CSF AD biomarkers in clinical and prodromal cohort.

Diagnostic category	CSF tested, n.	CSF A+, %	CSF T+, %	CSF N+, %
Clinical cohort				
DLB	34	32.4	14.7	14.7
AD	43[a]	90.6	100	76.7
PSP/CBS	30	13.3	3.3	0
MSA	31	6.4	3.2	9.7
PD	70	14.3	5.7	2.8
Clinical controls	29[b]	0	6.8	3.4
Prodromal cohort				
PAF	28	22.2	0	0
iRBD	18	16.7	11.1	11.1
MCI-LB				
● ISNB	45	22.2	6.7	11.1
● VUmc	35[b]	48.5	51.4	34.3
MCI-AD				
● ISNB	58	100.0	94.8	79.3
● VUmc	62	100.0	90.3	88.7
Unsp-MCI	30	10.0	16.7	16.7
SCD/CTRL				
● ISNB	30	0	0	0
● VUmc	28	0	53.5	42.8
Probable AD cohort	206[a]	95.1	88.3	85.9

ATN classification according to the following criteria: ISNB cohort (including clinical cohort): A+ Aβ42/40 ratio <0.68, T+ p-tau >58 pg/ml, N+ t-tau >450 pg/ml; VUmc: for Innotest A+ Aβ42 < 813 pg/ml, T+ p-tau > 52 pg/ml, N+ = t-tau > 375; for Elecsys A+ Aβ42 < 1000 pg/ml, T+ p-tau > 18, N+ t-tau > 235. [a] Patients with an amyloid-beta 1-42:amyloid-beta 1-40 (Aβ42:Aβ40) ratio of 0.68 or higher showed decreased Aβ42 levels combined with increased total (t)-tau and phospho (p)-tau concentrations (T+,N+) in CSF or abnormal p-tau:Aβ42 or t-tau:Aβ42 ratio. One case in the probable AD cohort carried a mutation in presenilin. [b] Data available in 35 out of 62 (clinical controls) and 35 out of 36 patients (MCI-LB VUmc).

Neuropathological studies

Neuropathological examination was performed using standardized procedures according to the autopsy protocol of the Laboratory of Neuropathology at ISNB (113). Briefly, the brain is sagittally

divided in the two hemispheres: the left half is fixed in 10% buffered formalin while the right one is sectioned coronally and then immediately frozen at − 80 °C in sealed plastic bags. Once formalin-fixed, the left hemibrain is serially sectioned in 1 cm slices, and regionally sampled in tissue blocks according to standardized procedures (151).

Seven µm thick sections from each block were stained with hematoxylin-eosin for screening. Moreover, immunohistochemistry with antibodies specific for α-Syn (LB509, dilution 1:100, Thermo Fisher Scientific, and KM51, dilution 1:500, Novocastra), hyperphosphorylated tau (AT8, dilution 1:100, Innogenetics), Aβ (4G8, dilution 1:5000, Signet Labs), and PrP (3F4, dilution 1:400, Signet Labs) was applied to all cases using several brain regions, mainly following established consensus criteria (152-155). An experienced neuropathologist (Prof. Piero Parchi) formulated the final diagnosis, assigned the Braak stage of LB-related pathology (155), and classified each case according to the level of AD neuropathologic change (ABC score) [152, 154].

CSF collection and analyses

CSF samples were obtained by LP at the L3/L4 or L4/L5 level following a standard procedure both at ISNB and at VUmc. Specimens were centrifuged in case of blood contamination, divided into aliquots, and stored in polypropylene tubes at −80 °C until analysis.

At ISNB, CSF t-tau, p-tau, Aβ42, and Aβ40 were measured by automated chemiluminescent enzyme immunoassay (CLEIA) on the Lumipulse G600 platform (Fujirebio, Gent, Belgium). The Aβ42:Aβ40 ratio was calculated as previously described(156). At VUmc, CSF Aβ42, p-tau and t-tau concentrations were determined using Innotest enzyme-linked immunosorbent assays (ELISA) (Fujirebio) or Elecsys assays (Roche Diagnostics, GmbH, Mannheim, Germany) run on the Cobas e601 analyzer (Roche Diagnostics, Basel, Switzerland) (157). Pathological values for the AD core markers were determined according to internally validated cut-off values at both centers (157-159).

Storage and extraction of plasmid DNA and bacterial transformation

pET28a+ plasmids carrying His-tagged wild type (wt) human α-Syn were donated by Dr. Byron Caughey's lab. To better preserve the DNA quality, pET28a+ plasmids were maintained in endA deficient NEB 5-α *E. coli* transformed following the protocol supplied by the company (New England BioLabs, NEB). Briefly, 1 µl of 2 ng/µl plasmid DNA was added to 50 µl of just thawed cells.

The tube was carefully flicked 3-4 times and incubated for 30 minutes on ice. Then, a heat shock was performed at 42 °C for exactly 30 seconds and cells were re-incubated for 5 minutes on ice. After that, 950 µl of room temperature SOC were added to the tube before a 60 minutes incubation at 37 °C on vigorous shaking (250rpm). Fifty µl of the grown culture were then 10-fold serially diluted, spread on selection plate with 50 µg/ml kanamycin (Kan) and incubated overnight at 37°C. The next day, a single colony was inoculated in LB broth for a 4-6 hours incubation at 37 °C and 250 rpm. When the ideal optical density (OD) was reached (0.6-0.8) the bacteria were stored in 15% glycerol stock at -80 °C.

At the first need, the conserved bacteria were picked with an inoculation loop and incubated overnight in a new Kan+ starter culture. Fresh plasmid DNA was finally extracted from NEB 5-α *E. coli* following the manufacturer's protocol (QIAprep Spin Miniprep Kit (50) 27104, Qiagen).

Competent BL21 (DE3) (C2527H, New England BioLabs) bacteria were transformed with wild-type (wt) human α-Syn plasmid following the protocol described above. To improve transformation efficiency, the heat shock step consisted of 10 sec instead of 30 sec at 42°C as previously indicated. The colonies grew in selective plates were immediately inoculated in fresh LB broth to proceed with a new purification or make fresh 15% glycerol stocks.

Purification of human recombinant α-Syn

The purification of the recombinant α-Syn was performed as reported (130), with minor modifications. Briefly, BL21 (DE3) bacteria from glycerol stock were streaked on a selective plate (Kan+, 50 µg/ml) and incubated overnight. Subsequently, a well isolated single colony was inoculated into 5 ml of Luria Broth (LB, Sigma) with kanamycin (Sigma) and let grow for 4–5 h at 37 °C with continuous agitation at 250 rpm. The starter culture was then added to 1 L of LB containing kanamycin plus the overnight express auto-induction system (Merk-Millipore 71300-4) in a fully baffled flask. Cells were grown in a shaking incubator at 37 °C, 200 rpm overnight. The next day, the culture was divided into four 250 ml flasks and centrifuged at 3200 × *g* for 10 min at 4 °C. The pellet was gently re-suspended in 25 ml osmotic shock buffer containing 40% sucrose, 2 mM EDTA, and 30 mM Tris at pH 7.2 using a serological pipette and incubated 10 min at room temperature under mild agitation on a rotator mixer. Next, the suspension was centrifuged at 9000×*g*, 20 min at 20 °C and each pellet was resuspended in 10 ml of ice-cold water. Successively, the suspensions were pooled into two 50 ml tubes and 20 µl of saturated $MgCl_2$ was added to

each 20 ml suspension. After an incubation of 3 min under mild rocking on ice, the suspension was centrifuged at 9000×*g*, 30 min at 4 °C. The pellet was discarded and the supernatant collected into a 100 ml glass beaker containing a magnetic stir bar. The pH was reduced to pH 3.5 by adding 400–600 µl HCl 1 M and incubated under stirring for 10 min at room temperature. A second centrifugation at 9000×g for 30 min at 4 °C was performed and the supernatant was collected into a fresh 100 ml glass beaker containing a magnetic stir bar. The pH was adjusted to 7.5 by adding 400–600 µl NaOH 1 M. The protein extract was filtered through a 0.22 µm filter (Merk-Millipore), loaded into a Ni–NTA column (Cytiva 17525501) on an NGC chromatography system (Bio-Rad) and washed with 20 mM Tris, pH 7.5 at room temperature. The column was further washed with 50 mM imidazole in Tris 20 mM, pH 7.5, generating a peak that was not collected. A linear gradient up to 500 mM imidazole in 20 mM Tris, pH 7.5 was performed, and the peak was collected between 30 and 75% of imidazole buffer (150 and 375 mM, respectively). This peak was loaded onto an anion exchange column Q-HP (Cytiva 17115401) and washed in Tris 20 mM, pH 7.5, followed by another washing in 100 mM NaCl in Tris 20 mM, pH 7.5. Again, a linear gradient up to 500 mM of NaCl in Tris 20 mM pH 7.5 was carried out to collect the peak between 300 and 350 mM NaCl. The obtained fractions were pooled and filtered through a 0.22 µm filter and dialyzed against water overnight at 4 °C using a 3.5 kDa MWCO dialysis membrane (Thermo-Scientific). The next day, the protein was moved into fresh water and dialyzed for four more hours. The protein concentration was measured with a spectrophotometer using a theoretical extinction coefficient at 280 nm of 0.36 (mg/ml)-1/cm. Finally, the protein was lyophilized using a lyophilizer (Thermo-Scientific) for 6 h and stored in aliquots at a final concentration of 1 mg/ml once re-suspended into 500 µl of phosphate buffer (PB) 40 mM, pH 8.0. Lyophilized aliquots were stored at − 80 °C until usage.

α-Syn RT-QuIC

Black 96-well plates with a clear bottom (Nalgene Nunc International) were pre-loaded with six 0.8 mm silica beads (OPS Diagnostics) per well. CSF samples were thawed and vortexed 10 s before use. Fifteen µL of CSF were added as seed to trigger the reaction in 85 µL of buffer containing 40 mM PB, pH 8.0, 170 mM NaCl, 10 µM thiofavin-T (ThT), 0.0015% sodium dodecyl sulfate (SDS), and 0.1 mg/ml of recombinant α-Syn filtered using a 100 kDa MWCO filter (Pall-Life Sciences). The plate was sealed with a plate sealer film (Nalgene Nunc International) and

incubated into Fluostar Omega (BMG Labtech) plate reader at 42 °C with intermittent double orbital shaking at 400 rpm for one minute, followed by 1-min rest. ThT fluorescence measurements were taken every 45 min using 450 nm excitation and 480 nm emission filter to overcome possible batch-to-batch variations of α-Syn activity and intrinsic plate-to-plate experimental variability, relative fluorescent units (RFU) for every time point were normalized for the maximum intensity reached by the positive control and expressed in percentage.

Samples were run in quadruplicates and deemed positive when at least 2 out of 4 replicates reached the threshold. The latter was calculated as the average normalized fluorescence value of NP negative control replicates during the first 10 hours of all runs, plus 30 standard deviations. The cut-off was set-up at 30 hours. When only one replicate crossed the threshold, the analysis was considered "unclear" and repeated up to three times. All RT-QuIC experiments were performed at ISNB by personnel blinded to the clinical diagnostic group.

Statistical analysis

We performed statistical analysis and plot fluorescence values expressed by the α-Syn RT-QuIC with GraphPad Prism 8.4 software (La Jolla, CA) . The time required to reach the threshold (lag phase), maximum intensity of fluorescence (Imax), and area under the curve (AUC) were extracted for each sample replicate. Depending on the data distribution, the Mann-Whitney U test or t test (continuous variables) and the $\chi 2$ test or Fisher exact test (categorical variables) were used, as appropriate, to test for differences between 2 groups. One-way analysis of variance (ANOVA) or Kruskal-Wallis test followed by Tukey or Dunn post hoc test were instead used to compare multiple groups. The analysis of coefficient of variation (CV) was performed to test the intra- and inter-batch variability. Statistical significance was set at $p < 0.05$. To assess the assay performance in discriminating the study groups, we calculated the sensitivity, specificity, positive and negative predictive values, and diagnostic accuracy, first in each study cohort and then in the whole population. To consider the cluster data structure, when evaluating the same discriminatory capacity in the combined cohorts, we applied a mixed-effects logistic regression model with the cohorts as the group variable. The likelihood ratio test revealed no significant differences between the mixed-effect model and a classic logistic regression model, thereby excluding a significant cluster effect. Finally, because we classified the clinical state of patients with MCI-LB only after

follow-up, to rule out potential bias, we also calculated the assay sensitivity in the MCI-LB group including only cases with a probable diagnosis at LP.

RESULTS

Setting-up of α-Syn RT-QuIC

Purification of recombinant α-Syn

For the production and purification of recombinant α-Syn, we followed the protocol described by Groveman et al. (127, 160). However, the protocol efficiency needed validation, given that differences in the operators and consumable materials could generate altered products unsuitable for the assay. Moreover, devices such as the chromatography system and the freeze-drier could be crucial for protein quality.

After identifying the best transformation efficiency, we faithfully reproduced the protocol (160) in the LabNP with a protein yield of about 15 mg per liter of bacterial culture. The chromatograms resulting from the two sequential column purifications and the collected fractions are illustrated in figure 3. The α-Syn recombinant protein was finally successfully lyophilized.

Assay reproduction

To set-up the α-Syn RT-QuIC, we carried out a pilot experiment including four probable DLB cases and four neuropathologically confirmed control cases (two affected by AD, one by encephalitis, and one by carcinomatosis) following the protocol described by Groveman et al. (127). Firstly, we tested the assay with a batch of recombinant α-Syn (RML WT α-Syn) generously donated by Dr. Caughey (TSE/Prion Biochemistry Section, Laboratory of Persistent Viral Diseases, NIAID, NIH) and, secondly, using our first recombinant product (ISNB WT α-Syn). Both analyses demonstrated α-Syn seeding activity in all replicates of probable DLB samples and a negative outcome in the control cases (figure 4).

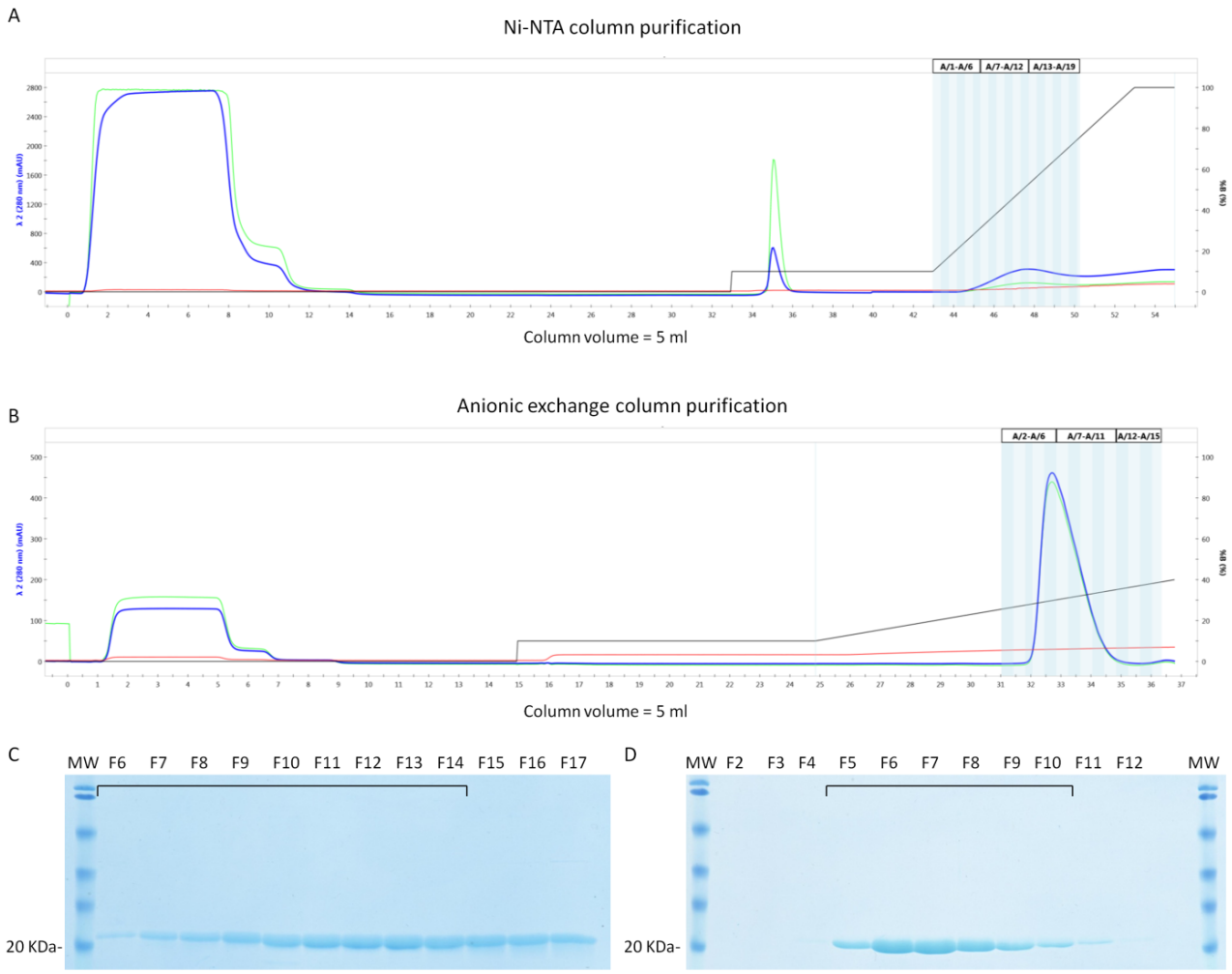

Figure 3. Purification of WT recombinant α-Syn by NGC chromatographic system. A) Chromatogram of Ni-NTA column purification and relative protein peak at the gradient elution step with imidazole buffer. B) Chromatogram of anionic exchange column purification and relative protein peak at the gradient elution step with saline buffer. The lines are illustrated as follows: green, absorbance at 260 nm; blue, absorbance at 280 nm; red, conductivity; black, percentage of buffer B. C) and D) show the fractions (F) collected from the first and the second peak, respectively. Only the fraction included in the black square bracket were processed for the following steps. MW = marker, molecular weight.

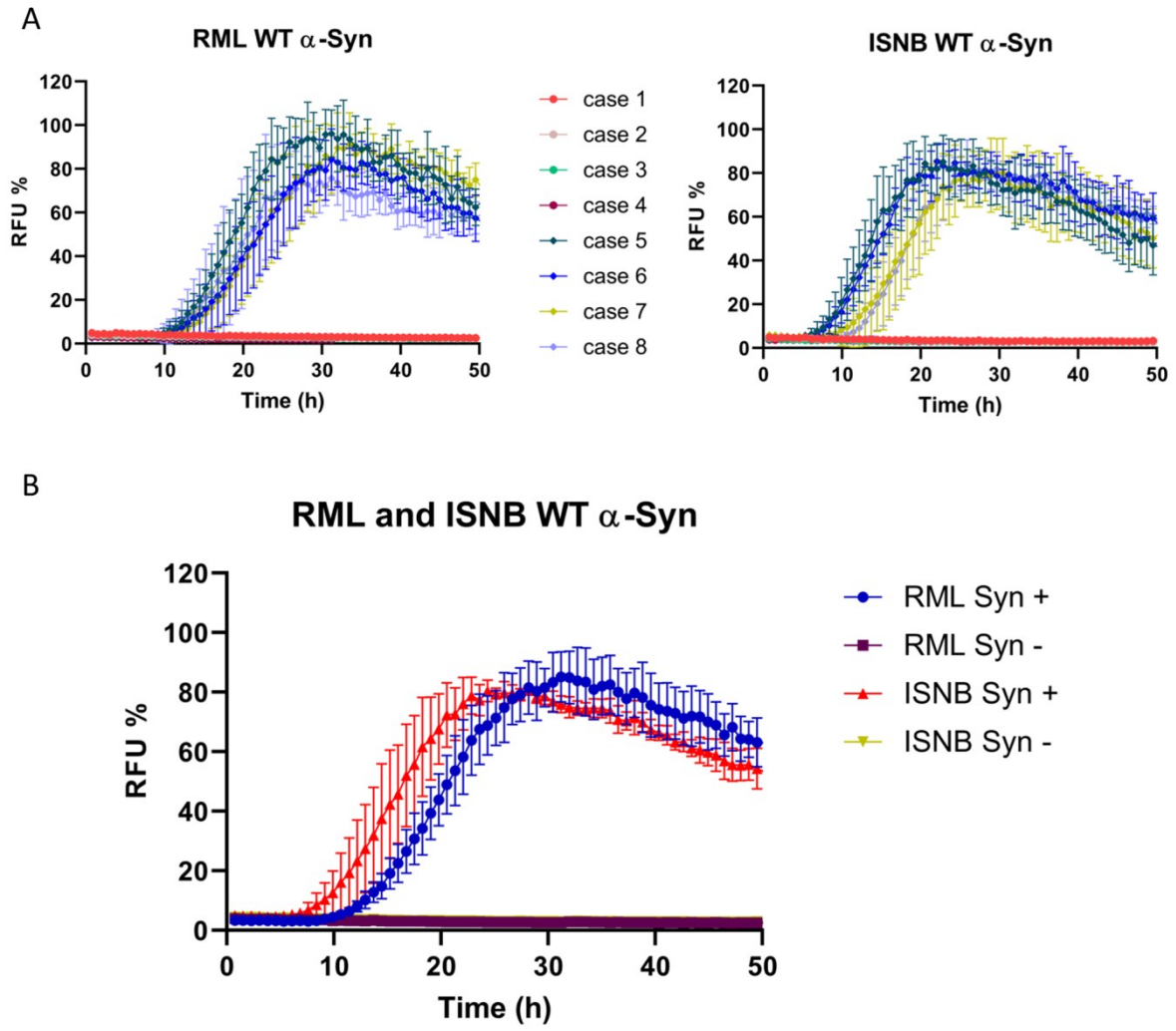

Figure 4. α-Syn RT-QuIC assay setting-up and WT recombinant α-Syn comparison. A) RML and ISNB WT α-Syn comparison of the tested control cases (case 1, 2, 3, and 4) and probable DLB cases (case 5, 6, 7, and 8). The values are expressed as the mean of four replicates per each case. B) Mean of all RFU values relative to the positive and negative groups tested with the two recombinant proteins. Syn+=sample positive to α-Syn RT-QuIC; Syn-=sample negative to α-Syn RT-QuIC; RFU=relative fluorescence unit (expressed as percentage after normalization)

Validation of α-Syn RT-QuIC with neuropathologically assessed cases

Following the preliminary set-up, we extended the analysis to CSF samples from 21 subjects demonstrating various extents of LB-related pathology at post-mortem examination (i.e.; Braak stage 1–6, Fig. 5) and 121 subjects lacking LB-related pathology. The CSF α-Syn RT-QuIC yielded an overall sensitivity of 95.2% and a specificity of 99.2% (table 3 and figure 6a). Despite the absence of any detectable α-Syn deposits, one case with a primary neuropathological diagnosis of

Wernicke's encephalopathy showed an unexpected positive result. Interestingly, 100% (14/14) of patients analyzed with definite DLB showed a positive response to the assay (table 3).

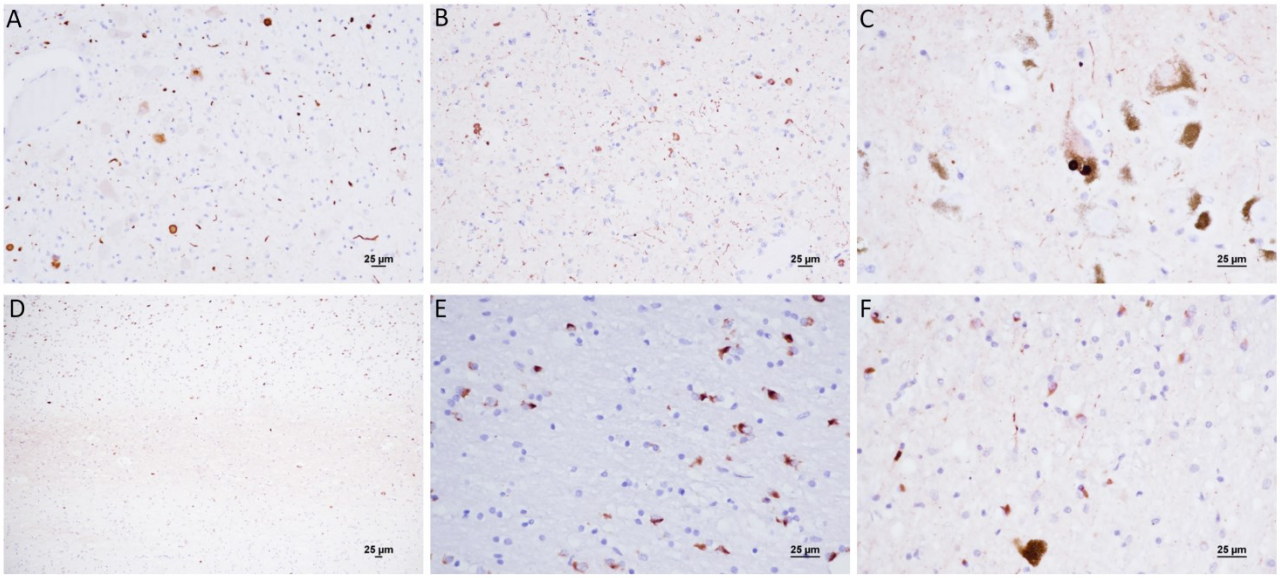

Figure 5. Distinctive α-Syn pathology evaluated by immunostaining. Characteristic aggregation of α-Syn in (A-C) DLB and (D-F) MSA subjects. A) Diffuse Lewy bodies and Lewy neurites in medulla and B) amigdala. C) LB inclusions in the neurons of substantia nigra. D) Glial cytoplasmic inclusions (GCIs) differently dispersed in grey and white matter of insula; GCIs involving E) striatum and F) substantia nigra areas.

Table 3. Sensitivity and specificity of α-Syn RT-QuIC across the "NP" and "clinical" cohorts.

Diagnostic category	n	Pos.	Neg.	Sensitivity	Specificity
Definite NP cohort					
LB α-Syn +	21	20	1	**95.2%**	
• Definite DLB	14	14	0	100%	
• Dementia with incidental LB	7	6	1	85.7%	
LB α-Syn -	121	1	120		**99.2%**
• AD	18	0	18		100%
• PSP	1	0	1		100%
• MSA	2	0	2		100%
• Syn- controls	100	1	99		99%
Clinical cohort					
LB α-Syn +	104	99	5	**95.1%**	
• DLB	34	33	1	97.1%	
• PD	70	66	4	94.3%	
LB α-Syn –	166	10	156		**94.0%**
• AD	43	7	36		83.7%
• Clinical controls	62	1	61		98.4%
• PSP/CBS	30	0	30		100%
• MSA	31	2	29		93.5%
All LB-related synucleinopathies*	125	119	6	**95.2%**	

Pos=positive; Neg=negative; LB α-Syn +=diagnostic group with LB-related pathology; LB α-Syn -=diagnostic group without LB-related pathology. Bold symbol highlights the sensitivity of the assay in the two most significant diagnostic groups and its specificity against the LB-related α-Syn negative controls

[a] Include neuropathologically confirmed and clinical cases.

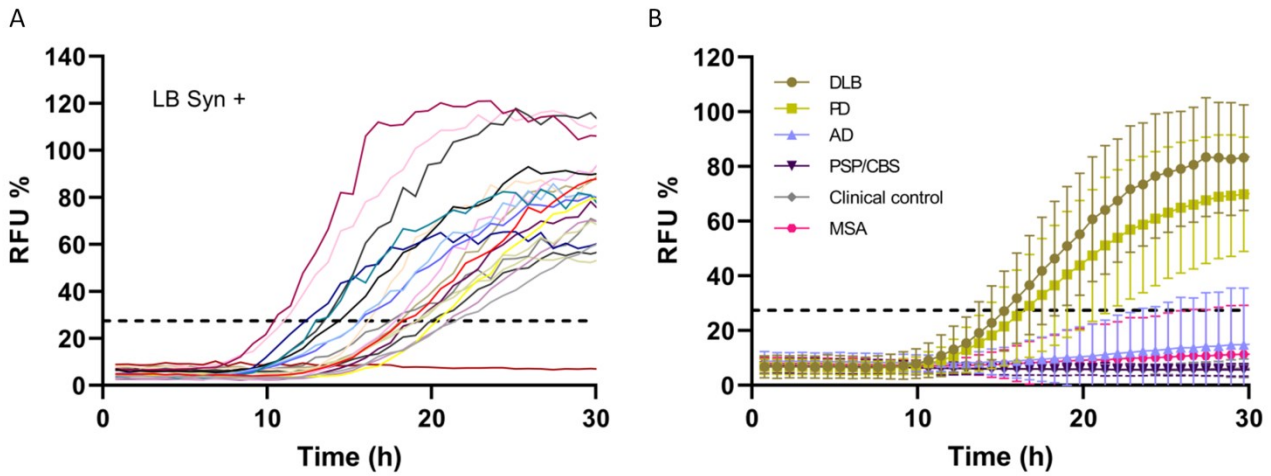

Figure 6. Kinetic curves of α-Syn seeding activity measured by RT-QuIC. A) Seeding activity observed in 20 out of 21 of neuropathologically confirmed LB α-Syn+ cases. Each curve depicts the average of quadruplicates. Standard deviation (SD) was hidden to make the image more readable. B) Kinetic curves detected in the different diagnostic groups of the "clinical" cohort. Each curve represents the average of the group, error bars indicate the SD, and the black dashed line indicates the threshold.

Diagnostic performance of α-Syn RT-QuIC in the "clinical" group

We subsequently evaluated the diagnostic value of α-Syn RT-QuIC in 270 cases with a probable or clinically established diagnosis (table 3 and figure 6b). Positive results were obtained in almost all DLB and PD patients, confirming α-Syn seeding activity in 95.1% of LB-related synucleinopathies (LB α-Syn +). The analyzed subjects who tested positive by RT-QuIC included 76 participants (76.8%) with a complete 4/4 (4 out of 4 positive replicates) positive response, 12 (12.1%) with 3/4, and 11 (11.1%) with 2/4 (table 4). We also detected a positive α-Syn seeding activity in a minority of subjects belonging to the clinical groups not typically associated with LB pathology (i.e., AD, PSP/CBS, MSA, and clinical control). Indeed, the α-Syn RT-QuIC showed a positive outcome in 6% of these patients, falling to 2.4% after the exclusion of the AD cases. Notably, we had only one positive test among the 62 control cases, resulting in an assay specificity of 98.4%. Overall, the

assay displays 99.0% PPV, 91.0% NPV, and 95.8% diagnostic accuracy in identifying LB syn+ against clinical controls.

The observed differences in the α-Syn RT-QuIC response induced us to further explore the kinetic parameters that may better reflect the heterogeneity of the α-Syn seeding reaction and discriminate between disease groups.

Table 4. **Percentage of α-Syn RT-QuIC positive replicates across the diagnostic categories of "clinical" group.**

Diagnostic categories	**N of positive wells (samples, n)** **%**		
LB α-Syn + n=99	2 (11) **11.1%**	3 (12) **12.1%**	4 (76) **76.6%**
PD n=66	2 (10) **15.1%**	3 (11) **16.7%**	4 (45) **68.2%**
DLB n=33	2 (1) **3.0%**	3 (1) **3.0%**	4 (31) **94.0%**
LB α-Syn – n=10	2 (3) **30%**	3 (3) **30%**	4 (4) **40%**
AD n=7	2 (2) **28.6%**	3 (3) **42.8%**	4 (2) **28.6%**
MSA n=2	2 (0) **0%**	3 (0) **0%**	4 (2) **100%**
Clinical control n=1	2 (1) **100%**	3 (0) **0%**	4 (0) **0%**

LB α-Syn +=diagnostic group with LB-related pathology; LB α-Syn -=diagnostic group without LB-related pathology.

Definition of kinetic parameters and assay reproducibility

Before proceeding with a more detailed analysis, we aimed to define further the parameters that describe the kinetic reaction and verify the assay reproducibility. To this aim, after an appropriate normalization and threshold definition based on previous prion RT-QuIC studies (112, 161), we choose the following three parameters:

- Lag phase: the time required by the fluorescence reaction curve to reach the threshold

- Imax: maximum fluorescence intensity value reached by the curve
- AUC: area under the curve

The details are illustrated in the figure 7.

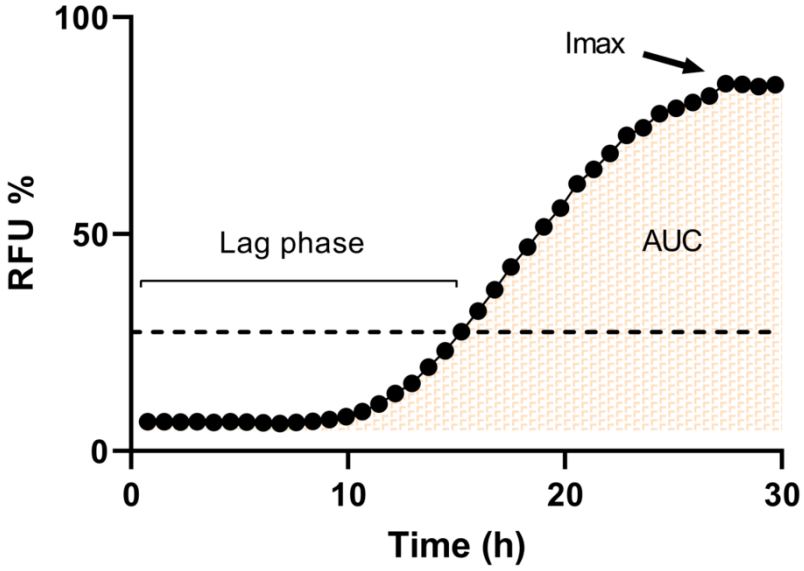

Figure 7. α-Syn RT-QuIC kinetic parameters.
Graphical representation of lag phase, Imax and AUC (area under the curve).

To verify the assay reproducibility, we explored the intra-batch and batch-to-batch variations of α-Syn RT-QuIC by analyzing the three kinetic parameters. For this purpose, we compared the kinetic curves of the same positive control using eight different batches of recombinant protein. The intra-batch coefficient of variation (CV) of the Lag phase varied between 13.4% and 29.4% (median=13.7%). Analogously, the Imax and AUC varied between 5.1% and 18.9% (median=13.7%) and 14.8 and 40.4% (median=13. 7%), respectively. No statistically significant differences were observed in the inter-batch analysis (Lag phase, p=0.307; Imax, p=0.517; AUC, p=0.103) (figure 8).

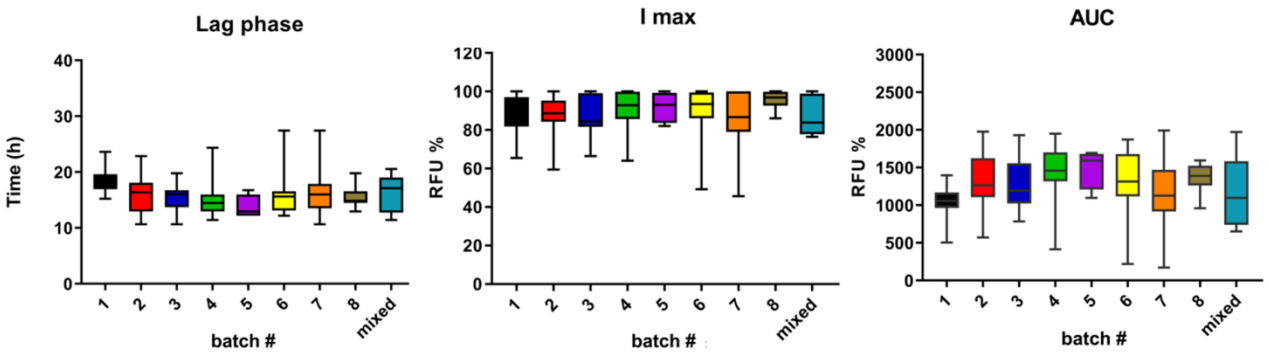

Figure 8. Batch-to-batch and intra-batch variation of fluorescence signal induced by recombinant α-Syn aggregation in the RT-QuIC. Lag phase, Imax and AUC of the same positive control tested with different batches of recombinant α- Syn. Each colour depicts the performance of a different batch of α-Syn. In the other graphs, error bars represent intra-batch variability, calculated for positive control on, respectively 2 (batch #1), 4 (batch #2), 4 (batch #3), 6 (batch #4), 1 (batch #5), 2 (batch #6), 8 (batch #7), 2 (batch #8), and 2 runs (mixed batches #2 + #6, and #7 + #8). Differences in the dimension (n) of the runs per batch were related to the variability in the yield of recombinant α-Syn between batch preparations.

In a total of 413 (neuropathological and clinical cohorts) analyzed samples, an unclear result (one positive well) occurred 28 times (6.8%), and in most cases (85.7%) involved samples yielding a negative outcome at the second test (table 5). Finally, 13 out of 16 (81.3%) positive samples that we tested three times using different substrate batches confirmed the positive result of the first run in both repetitions (table 6). The only exception was represented by three samples with a two out of four positivity. Two gave unclear results in the second run but confirmed the positivity in the third one, while a third sample gave a one out of two as the third result after two positive outcomes. However, changes in the diagnostic decision (positive vs. negative) did not occur.
These findings allowed us to proceed with a more detailed analysis of the “clinical” subgroups.

Table 5. **Percentage of "unclear" results across the neuropathological and clinical cohort.**

Diagnostic categories	Unclear/Total runs (%)	Final result of repeated test	
		0/4 (%)	**≥2/4 (%)**
Syn –	25*/ 287 (8.7)	14 (93.3)	1 (6.7)
Syn- NP controls	7* / 100 (7.0)	7	-
Clinical controls	5 / 62 (8.1)	4	1
PSP/CBS	3 / 31 (9.7)	3	-
AD	5 / 61 (8.2)	3	2
MSA	5 / 33 (15.2)	5	-
Syn +	3* / 126 (2.4)	2 (66.7)	1 (33.3)
Syn+ NP controls°	2* / 7 (28.6)	1	1
PD	1 / 71 (1.4)	1	-
Total	28 / 413 (6.8)	24 (85.7)	4 (14.3)

° Dementia with incidental LB *One sample needed a further repetition because of a second unclear result.

Table 6. Evaluation of result reproducibility by multiple runs.

		First result					
		2/4 (n=6*)		**3/4 (n=2†)**		**4/4 (n=8§)**	
Diagnostic groups		Second result (%)	Third result (%)	Second result (%)	Third result (%)	Second result (%)	Third result (%)
LB - syn + (syn+ NP, DLB, PD)	0/4	-	-	-	-	-	-
	1/4	2 (33.3)	1 (20.0)	-	-	-	-
	2/4	2 (33.3)	2 (40.0)	-	-	-	-
	3/4	1 (16.7)	1 (20.0)	1 (50.0)	-	-	3 (37.5)
	4/4	1 (16.7)	1 (20.0)	1 (50.0)	2 (100)	8 (100)	5 (62.5)

*Includes 4 PD, 1 DLB and 1 syn+ NP; † Includes 2 PD; § Includes 4 PD and 4 DLB. NP = neuropathological

α-Syn RT-QuIC in patients with parkinsonism

We detected a consistent positive seeding activity in PD, but not in PSP/CBS, clinical neurological controls, and, unexpectedly, MSA. Specifically, the assay demonstrated 94.3% sensitivity in the probable PD cohort, 98.4% specificity against the clinical control, 100% against patients with PSP/CBS and 93.5% against those with MSA. Incongruent results were limited to four out of 70 with PD who tested negative and two out of 31 patients with probable MSA who showed α-Syn seeding activity (table 2). A detailed analysis of the clinical features of the three idiopathic PD

subjects negative to the assay, reveal a mild disease severity (baseline score at the UPDRS scale section III: 16, 14, and 8), and an isolated, unilateral tremor in two of them. Moreover, whereas all patients who carried GBA mutation tested positive, the only patient with LRRK2 mutation lacked α-Syn seeding activity, a result in line with a recent study demonstrating a much lower sensitivity of α-Syn RT-QuIC in LRRK2-PD than in idiopathic PD (126). Among the 66 α-Syn RT-QuIC positive PD, the positive replicate response was distributed as follows: 45 (68.2%) 4/4, 11 (16.7%) 3/4, and 10 (15.1%) 2/4. The two positive MSA showed a complete reactivity in all replicates (table 4). Finally, we found no statistically significant differences in the lag phase (PD 18.0±4.4 and MSA 18.4±5.6; p=0.819, Imax (PD 87.3±25.7 and MSA 80.9±29.5; p=0.496), and AUC (PD 892.5±425.3 and MSA 780.8±476.5; p=0.469) between the positive patients of the two cohorts.

α-Syn RT-QuIC in patients with dementia

After the striking results obtained in the "neuropathological" group, we further evaluated the assay's performance in the “clinical group” by examining the probable DLB and AD. By detecting a seeding activity in 97.1% (33/34) of probable DLB patients, we obtained an almost complete concordance between the DLB neuropathological and clinical cohorts. In contrast, a higher positivity rate than in the neuropathological cohort was observed in the probable AD patients, which resulted positive in 16.3% of cases. Of the DLB patients who showed seeding activity, 31 gave a positive outcome in 4/4 (94.0%) replicates, 1 in 3/4 (3.0%), and 1 in 2/4 (3.0%). Instead, a different ratio of α-Syn RT-QuIC positive replicates was observed in AD group, where a 4/4, 3/4, and 2/4 positive response was found in 2 (28.6%), 3 (42.8%), and 2 (28.6%) patient, respectively (table 4). Although conditioned by a limited number of cases, a statistically significant difference between replicates distribution was observed ($p<0.001$). Finally, the comparison of the kinetic curves between the RT-QuIC positive DLB and AD patients showed statistically significant differences in all analyzed parameters: lag phase (DLB 17.0±3.8 and AD 20.2±4.9; $p<0.001$), Imax (DLB 92.6±23.8 and AD 79.6±25.1; p=0.023) and AUC (DLB 963.1±418.0 and AD 605.0±350.7; $p<0.001$). These differences between the two groups remained significant when the "neuropathological" cases were also considered in the DLB cohort.

Diagnostic performance of α-Syn RT-QuIC in the "prodromal" group

It is plausible that pathological α-Syn oligomers could develop years before disease onset. To study the phenomenon and explore the assay ability to predict the disease course, we studied prodromal synucleinopathies such as iRBD, PAF, and MCI-LB.

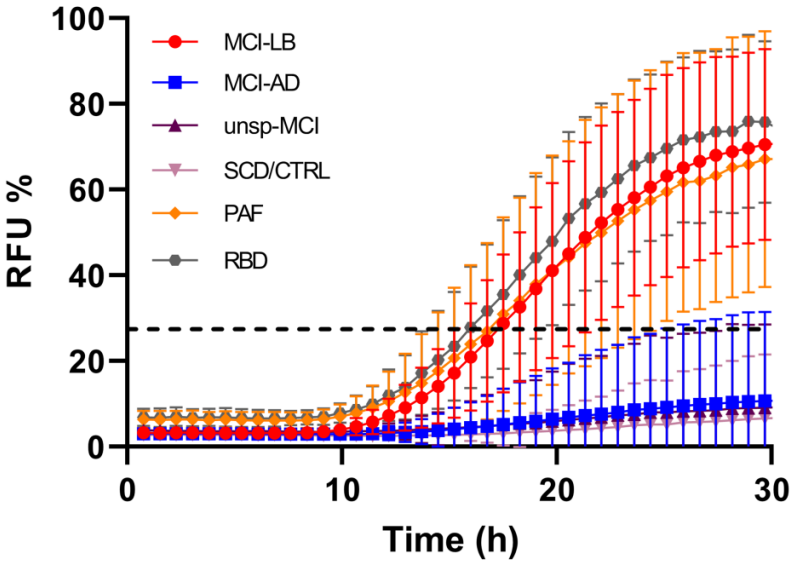

Figure 9. Kinetic curves of α-Syn seeding activity measured by RT-QuIC. Kinetic curves detected in the different diagnostic groups of the "prodromal" cohort. Each curve represents the average of the group, error bars indicate the SD, and the black dashed line indicates the threshold.

α-Syn RT-QuIC in patients with iRBD and PAF

In the analyzed iRBD cohort, 100% of patients (18/18) showed a positive outcome, with 4/4 positive replicates in 11 cases (61.1%), 3/4 in 5 (27.8%), and 2/4 in 2 (11.1%). Interestingly, one patient with the diagnosis of probable MSA at follow-up who had only RBD and AF at the time of LP tested negative by RT-QuIC. A negative result was also detected in 11 narcoleptic patients affected by RBD features (included in the clinical controls), resulting in a specificity of 100% towards this clinical mimic.

Similarly, with 25 out of 28 samples showing α-Syn seeding activity, the test sensitivity was 89.3% in the PAF cohort (table 7, figure 9). The distribution of the positive replicates across the runs was as follows: 67.9% 4/4, 14.3% 3/4, and 7.1% 2/4. Of note, one of the three PAF subjects who tested negative by RT-QuIC showed a clinical history relevant for intermittent diplopia and positivity for antiganglioside GQ1b antibody in serum. These two aspects indirectly suggest a possible underlying autoimmune etiology. At the same time, in a second negative patient, the normal adrenergic cardiac innervation at MIBG-SPECT, highlighting a clinical picture ascribable to MSA,

not to PD or DLB (162, 163). Finally, the last negative CSF was characterized by slight blood contamination, a pre-analytical factor likely interfering with the RT-QuIC reaction (164, 165).

Table 7. Sensitivity and specificity of α-Syn RT-QuIC across the "prodromal" cohort.

Diagnostic category	n	Pos.	Neg.	Sensitivity	Specificity
Prodromal cohort					
PAF	28	25	3	**89.3%**	
iRBD	18	18	0	**100%**	
MCI-LB	81	77	4	**95.1%**	
● ISNB	45	44	1	97.8%	
● VUmc	36	33	3	91.7%	
MCI-AD	120	16	104		**86.7%**
● ISNB	58	7	51		87.9%
● VUmc	62	9	53		85.5%
Unsp-MCI	30	2	28		**93.3%**
SCD/CTRL	58	2	56		**96.6%**
● ISNB	30	1	29		96.7%
● VUmc	28	1	27		96.4%

α-Syn RT-QuIC in patients with MCI

We detected α -Syn seeding activity in 95.1% of MCI-LB patients, with consistent percentages between the two analyzed cohorts: 97.8% and 91.7% in ISNB and VUmc cohorts, respectively. In comparison, 13.3% of MCI-AD revealed a positive α-Syn seeding activity, maintaining comparable percentages: 12.1% of the ISNB and 14.6% in VUmc patients. In contrast, 96.6% (56/58) control cases and 93.3% (28/30) of individuals with unsp-MCI showed a negative outcome (table 7, figure 9).

Comparing the kinetic curve parameters revealed a statistically significant difference in Imax between the MCI-LB and MCI-AD groups (83.4% vs 74.6%, p=0.002). In addition, we found a different proportion of positive replicates among the two groups, with samples giving 2 of 4 positive replicates more represented in the MCI-AD group than in the MCI-LB group (2/4: MCI-AD 25.0% vs. MCI-LB 3.9%, p=0.015) (figure 10).

Interestingly, whereas none of the two positive unsp-MCI showed any LB-related clinical features, either at the first evaluation or at follow-up, 6 of the 16 MCI-AD "positive" patients developed one

DLB clinical core feature at follow-up (i.e., visual hallucinations in four, and probable RBD in two), suggesting an underlying LB co-pathology. Furthermore, one additional subject in this group developed orthostatic hypotension, a supportive clinical criterion for DLB. In the RT-QuIC positive AD subgroup, 12 patients were classified as amnestic MCI (seven multidomain and five single domain) and four as non-amnestic (three multidomain, one single domain).

Overall, the assay displays 97.5% PPV, 93.3% NPV, and 95.7% diagnostic accuracy in identifying MCI-LB against controls, with a similar trend between the two cohorts.

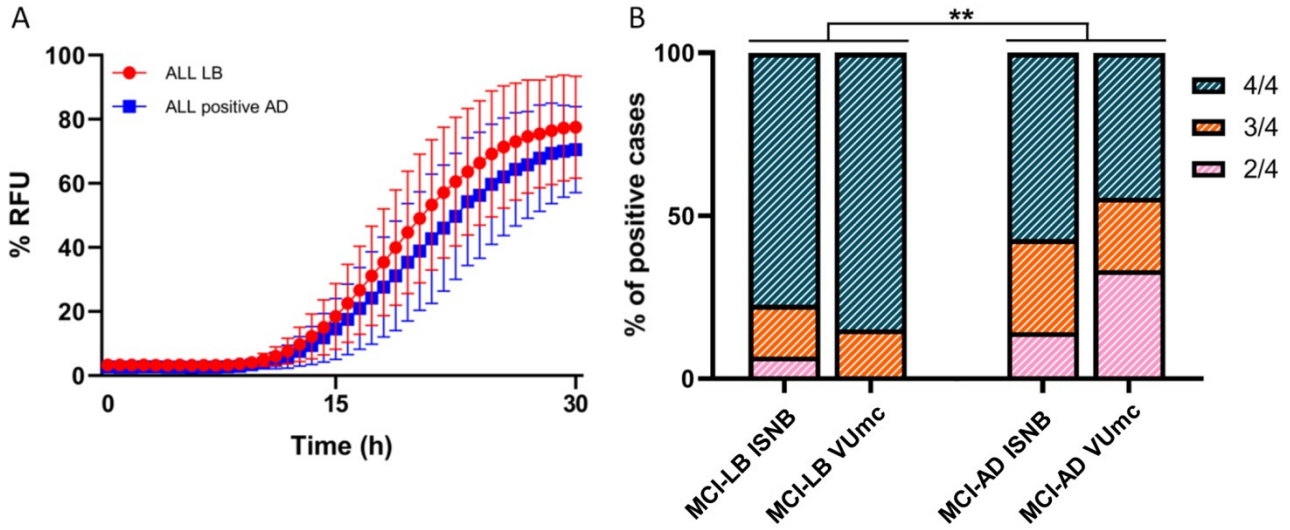

Figure 10. Comparison of α-Syn RT-QuIC positive patients among MCI-LB and MCI-AD groups. A) Kinetic curves comparison. Statistically significant differences between the 2 groups are limited to the maximum intensity of fluorescence (Imax) (**p<0.01). B) Analysis of positive replicates distribution in the MCI-LB and MCI-AD groups. Statistical analyses by the χ2 test resulted in **p<0.01. ns = non significant

Comparison of the α-Syn RT-QuIC results across prodromal MCI and probable DLB or AD

The α-Syn RT-QuIC ability to detect minute amounts of seeds in the early stage of disease and the slight but significant differences in the kinetic reaction seen between MCI-LB and MCI-AD suggested a more deepened analysis of RT-QuIC reactivity across the disease course. Pursuing the aim, we explored the kinetic parameters resulting from subjects affected by DLB, AD and compared them with those at the earlier MCI stage. Since the limited number of α-Syn RT-QuIC positive MCI-AD and AD patients (16 and 7 subjects, respectively) and to strengthen the analysis,

we further extended the analysis to 206 probable AD patients. The added cohort, which showed a positive outcome in 34 out of 206 cases (16.5%), in line with the results previously observed in the smaller group (table 3), was included in the investigation. Analogously, the DLB included both clinically and neuropathologically diagnosed patients. Intriguingly, we found statistically significant differences between MCI-LB and DLB groups (lag phase: 18.2±3.7 vs 17.05±4.1, p=0.004; Imax: 83.43±18.29 vs. 92.09±25.88, p<0.001; AUC: 849.9±333.8 vs 956.8±448.8, p=0.007), but not among MCI-AD and AD groups (lag phase: 19.7±4.8 vs 19.9±4.6, p=0.750; Imax: 77.7±18.0 vs 75.0±22.3, p=0.458; AUC: 760.0±351.5 vs 685.2±378.6, p=0.240). Moreover, whereas no statistically relevant differences were observed across the ratio of positive replicates along the disease course neither in LB-pathology (2/4: MCI-LB 4.2% vs. DLB 3.9%, p=0.209) or AD-pathology (2/4: MCI-AD 25.0% vs. AD 34.1%, p=0.437), discrepancy among DLB and AD enlarged cohort were confirmed (2/4: DLB 4.2% vs. AD 34.1%, p<0.001) (figure 11).

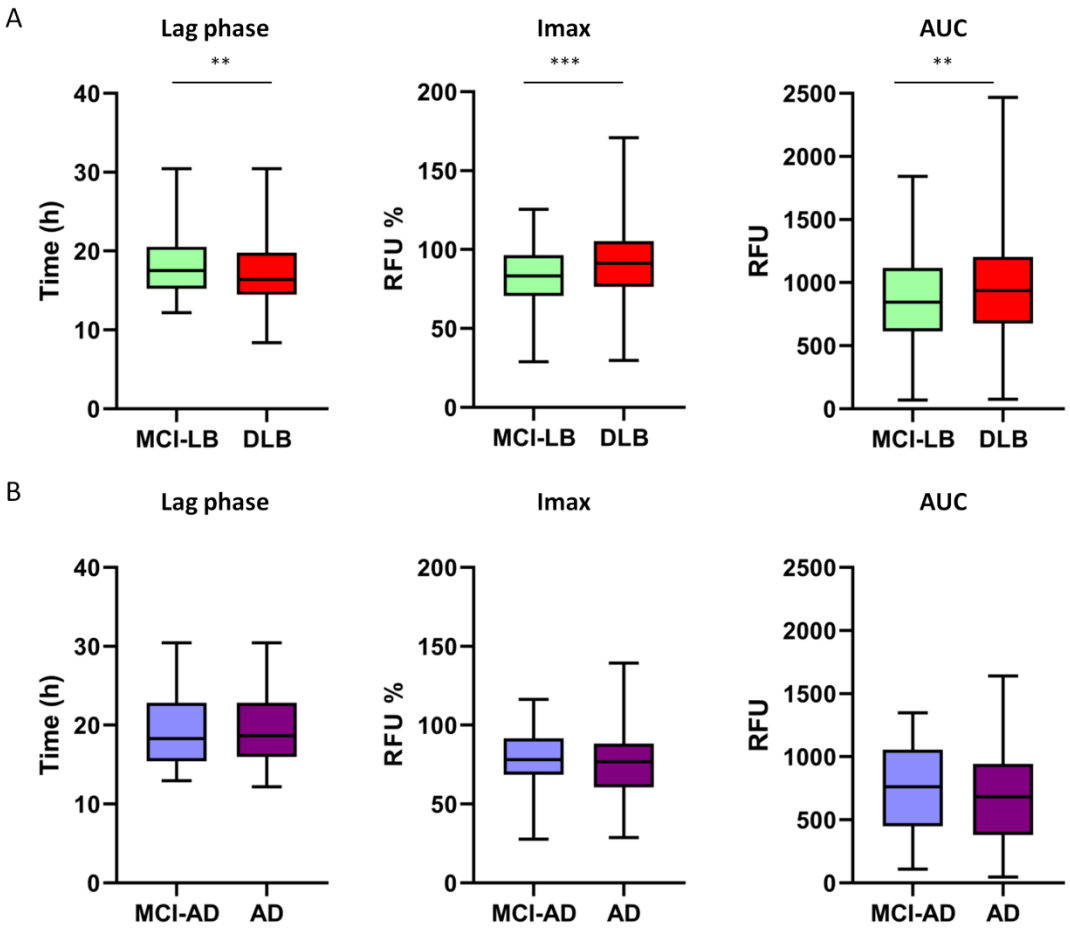

Figure 11. Analysis of kinetic parameters variations among prodromal MCI and DLB and AD cases. Lag phase, Imax and AUC were investigated in A) MCI-LB vs DLB and B) in MCI-AD vs AD. Statistically significant differences were found between MCI-LB and DLB in all analyzed parameters (**, p<0.01; ***, p<0.001).

DISCUSSION AND CONCLUSIONS

The overlapping symptoms across neurodegenerative diseases and the presence of pathological protein aggregate years before the disease onset implicate the urgent necessity of novel assays for an early and differential diagnosis of these disorders. Currently, the RT-QuIC represents one of the most promising approaches for providing pathology-specific biomarkers for neurodegenerative diseases. The capacity of RT-QuIC and other seeding amyloid assays (SAA) to amplify minute amounts of amyloid seeds permits an unprecedented sensibility and specificity for detecting the pathogenic neurodegenerative disease-related proteins in biological fluids. Pursuing a mechanism conceptually similar to DNA amplification by PCR, the RT-QuIC currently provides the highest expectation for a wide application in the diagnosis of neurodegenerative disorders, especially of those lacking reliable diagnostic biomarkers such as DLB, PD, and the frontotemporal lobar degeneration spectrum. Indeed, besides the studies that successfully implemented the α-Syn RT-QuIC, a few groups reported preliminary encouraging results also for the tau and TDP-43 RT-QuIC (166-168).

In the present work, the first challenge was to faithfully reproduce in the Laboratory of Neuropathology at ISNB the α-Syn RT-QuIC assay recently set up by Groveman and colleagues (127). The susceptibility of the RT-QuIC to several known and unknown reaction factors made the result uncertain. In particular, post-translational modifications during the protein expression and chemical contamination or physical alteration throughout the purification process could affect the α-Syn recombinant substrate and affect the assay performance. The critical role of the substrate has been underlined by several prion RT-QuIC studies, which showed the influence of the recombinant protein type on the performance of the diagnostic test as also highlighted by recent α-Syn RT-QuIC studies (127, 136, 169).

In the initial phase of the project, through a pilot study of assay reproducibility with limited and well-selected samples, we replicated the α-Syn RT-QuIC results obtained by Groveman et al. Also, we demonstrated the complete analogy between the RML WT α-Syn and our ISNB WT α-Syn recombinant protein. Taking advantage of the new promising assay, we then tested the largest neuropathologically verified cohort studied to date, obtaining an almost complete specificity (99.2%) and an unexpected sensibility (95.2%). We then extended the analysis to a well-characterized clinical cohort, including the whole spectrum of neurodegenerative parkinsonisms and two of the most common forms of neurodegenerative dementia. To this aim, we analyzed cohorts of patients with the clinical diagnosis of PD, PSP/CBD, MSA, DLB, and AD. Interestingly,

with the RT-QuIC readout, we could discriminate with very high sensitivity the PD and DLB cases from the tauopathies such as PSP and CBS.

Moreover, the assay also unexpectedly distinguished the PD cases from the non-LB-related synucleinopathies. Indeed, most CSF from MSA patients did not show any RT-QuIC response. In a previous work of this kind (170), the MSA cases showed a significantly lower positivity rate than the PD patients (35.2%, 6/17 positive cases). However, it was not as low as in our study. Using an α-Syn protein misfolding cyclic amplification (PMCA) assay, Soto's group initially discriminated PD (88.5%) and MSA (80%, 8/10 positive cases) patients from control and other neurodegenerative disorders (124). Subsequently, however, they were also able to discriminate the two diseases with an accuracy of 95% by exploiting the kinetic curve parameters of the assay (128). Similarly, despite a positive outcome in 9 out of 11 individuals with MSA, De Luca and co-workers reported that α-Syn aggregates generated from RT-QuIC reactions of samples obtained from the olfactory mucosa showed divergent biochemical and structural features between PD and MSA samples (132). Therefore, the explorable reasons behind the lack of detectable α-Syn seeding activity in MSA cases tested with our assay could embrace two aspects: “strain” specificity and the seeds amount in CSF. The former may be related to the difficulty of the α-Syn pathological protein conformer of MSA to convert the substrate and trigger the aggregation structurally. Notwithstanding the several findings that seem to suggest a significant seeding activity or infectivity in MSA strain (99), the RT-QuIC reaction environment could favor the selection of LB-related seeds. Finally, the presence of α-Syn aggregate in the form of GCI and, therefore, in a different cell population could lead to a scarce release of seeds. Based on previous seed dilution analysis on prion RT-QuIC (169-171), the delay of the lag phase in MSA cases observed in α-Syn PMCA may be attributed to such factor. However, to explain the LB-specificity of our assay, we cannot exclude the simultaneous influence of both hypothesized variables or other unconsidered causes.

On the basis of such observations, also the few discordant results deserve some comments. Indeed, among the well characterized PD cohort, four cases showed negative response to the assay. Whereas three idiopathic PD subjects were characterized by a mild disease, the fourth patient was instead a carrier of the G2019S mutation in *LRRK2* that, notoriously, is associated in some case with the lack of LB pathology (172). Moreover, the influence of pre-analytical variables (e.g. blood contamination, freeze-thawing cycles, etc.) on the failure of α-Syn seeding activity detection can not be excluded. Conversely, we detected α-Syn seeding activity in a neuropathologically confirmed case of Wernicke’s encephalopathy. Although no LB pathology was

detected by immunostaining in this patient, the analysis did not include the spinal cord, which can be an initial site of α-Syn accumulation.

The sensitivity of the assay could also explain the moderate α-Syn reactivity detected in AD patients. It has been shown in several studies that LB pathology may be found with relative frequency in the elderly population, even in the absence of neurological symptoms or signs (173-175). At the same time, LB co-pathology is frequently detected in patients with a clinical diagnosis of AD (176, 177). Remarkably, DeTure and colleagues demonstrated the presence of significant LB co-pathology compatible with a secondary diagnosis of DLB in 177 out of 626 (28%) AD subjects (178). Finally, we observed the same percentage of cases with α-Syn seeding activity in both the analyzed AD clinical cohorts [7/43 (16.3%) in the first one and 34/206 (16.5%) in the second one]. Together with our findings related to the neuropathologically verified cohort, this evidence suggests that AD cases with a positive RT-QuIC might also harbor LB, at least as significant co-pathology.

The outstanding performance of the α-Syn RT-QuIC, even in some cases with incidental focal LB pathology limited to the medulla, led us to explore further its diagnostic potential extending the analysis to the most characteristic prodromal syndromes associated with synucleinopathies: iRBD, PAF, and MCI.

We confirmed that the assay could quickly identify patients with LB-related synucleinopathies in the early phases of the disease with high accuracy. We were able to detect α-Syn seeding activity in 89.3% of PAF and 100 % of RBD, providing, once again, evidence that the two syndromes are mostly clinical manifestations of prodromal LB-related synucleinopathy. In particular, we noted that RT-QuIC negative PAF subjects came from individuals probably affected at follow-up by a non-LB-related pathology. In one 4-year prospective cohort, patients who manifested initially with PAF had a 34% risk to develop LBD or MSA, especially if they also had RBD (43). Similarly, PD or other synucleinopathies developed almost invariably in subjects with iRBD if they were followed up long enough (179, 180). Stefani and co-workers also tested olfactory mucosa of iRBD patients in α-Syn RT-QuIC, but with less promising results (44.4% of sensitivity and 89.8% of specificity). Nevertheless, other than using different tissue, the assay was carried out with an alternative protocol (181).

Moreover, in line with the findings relative to PAF and iRBD, we demonstrated that α-Syn RT-QuIC assay also accurately detects LB in CSF of MCI patients, indicating that, regardless of clinical presentation, patients with LB harbor significant α-Syn seeding activity early in the course of the

disease. The overall capability to distinguish MCI-LB reached 95.1% in the combined groups, whereas the specificity tested against cognitively unimpaired controls was 96.6%. Again, in almost complete accordance with the findings in the AD clinical cohort, 13.3% of MCI-AD showed a positive outcome. Interestingly, 7 of 16 cases (43.7%) developed at follow-up one or more DLB characteristic features, strengthen the hypothesis of a concomitant LB-pathology. As further evidence of the reliability of the data, the results obtained with the MCI ISNB cohort were widely comparable with those observed in the VUmc cohort.

Lastly, exploring the unsp-MCI group, the finding of α-Syn seeding activity in 6.7% of patients, is also consistent with the notion that 5-8% of people over 60 years old in the absence of extrapyramidal signs of cognitive decline are affected by incidental LB pathology (182, 183).

Although the positive or negative RT-QuIC output remains the primary criterion for a diagnostic evaluation, it appears evident as some pathologic groups showed different seeding reactions in terms of kinetic curve parameters or positive replicates. In particular, we observed statistically significant differences between clinically diagnosed DLB and AD in the lag phase, Imax, AUC, and the number of positive wells out of four replicates. In this case, the "quantity" rather than the "quality" of seeds may be at the origin of such discrepancies. The fact could easily explain the differences of kinetic parameters highlighted in the MCI-LB and DLB comparison, where, in parallel with the disease progression, an increase of LB and, consequently, seeds may occur. However, the maturity or type of seeds, in a dependent manner to the severity or group of pathology, should not be excluded.

Finally, with the present study, we demonstrated a promising and reliable application of α-Syn RT-QuIC to all LB-related synucleinopathies and relative prodromal phases, providing strong evidence of realistic employment in the diagnostic practice. Following the way traced by prion RT-QuIC, it is foreseeable that the assay will pursue the same course in a few years. However, the test still needs standardization and inter-laboratory validation, especially in light of substrates and protocol variability. Moreover, a more deepened analysis and protocol implementation will be required to further explore or develop the "quantitative side" of the α-Syn RT-QuIC, an aspect of evident utility in particular if correlated with the rate of disease progression. Indeed, in the era of the "prion-like theory," the quantification of seeding activity could represent a new frontier to predict the disease course and test drug efficacy.

The urgent need for specific biomarkers concerns the early diagnosis and clinical management of patients and extends to the design and outcome of clinical trials. In addition to searching for novel

therapies against α-Syn pathology in LB disease, the availability of an accurate early biomarker may improve patient selection in AD trials (184). Indeed, the co-occurrence of pathologies is notoriously considered a possible cause of therapeutic trial failures in neurodegenerative dementias (185, 186).

In conclusion, we think that the validation of the assay through translational studies in well-defined clinical and pathological cohorts is an important step forward for the early diagnosis of LB-related synucleinopathies. Indeed, with the demonstration, for the first time, of the actual applicability of RT-QuIC outside the prion field, the use of the assay for other pathologies became not only promising but also feasible.

BIBLIOGRAPHY

1. Maroteaux L, Campanelli JT, Scheller RH. Synuclein: a neuron-specific protein localized to the nucleus and presynaptic nerve terminal. J Neurosci. 1988 Aug;8(8):2804-15. doi: 10.1523/JNEUROSCI.08-08-02804.1988.
2. Gonçalves S, Outeiro TF. Assessing the subcellular dynamics of alpha-synuclein using photoactivation microscopy. Mol Neurobiol. 2013 Jun;47(3):1081-92. doi: 10.1007/s12035-013-8406-x. Epub 2013 Feb 8.
3. McLean PJ, Ribich S, Hyman BT. Subcellular localization of alpha-synuclein in primary neuronal cultures: effect of missense mutations. J Neural Transm Suppl. 2000;(58):53-63. doi: 10.1007/978-3-7091-6284-2_5.
4. Mori F, Tanji K, Yoshimoto M, Takahashi H, Wakabayashi K. Demonstration of alpha-synuclein immunoreactivity in neuronal and glial cytoplasm in normal human brain tissue using proteinase K and formic acid pretreatment. Exp Neurol. 2002 Jul;176(1):98-104. doi: 10.1006/exnr.2002.7929.
5. Uéda K, Fukushima H, Masliah E, Xia Y, Iwai A, Yoshimoto M, et al. Molecular cloning of cDNA encoding an unrecognized component of amyloid in Alzheimer disease. Proc Natl Acad Sci U S A. 1993 Dec 1;90(23):11282-6. doi: 10.1073/pnas.90.23.11282.
6. Jakes R, Spillantini MG, Goedert M. Identification of two distinct synucleins from human brain. FEBS Lett. 1994 May 23;345(1):27-32. doi: 10.1016/0014-5793(94)00395-5.
7. Bruening W, Giasson BI, Klein-Szanto AJ, Lee VM, Trojanowski JQ, Godwin AK. Synucleins are expressed in the majority of breast and ovarian carcinomas and in preneoplastic lesions of the ovary. Cancer. 2000 May 1;88(9):2154-63.
8. Polymeropoulos MH, Lavedan C, Leroy E, Ide SE, Dehejia A, Dutra A, et al. Mutation in the alpha-synuclein gene identified in families with Parkinson's disease. Science. 1997 Jun 27;276(5321):2045-7. doi: 10.1126/science.276.5321.2045.
9. Lee VM, Trojanowski JQ. Mechanisms of Parkinson's disease linked to pathological alpha-synuclein: new targets for drug discovery. Neuron. 2006 Oct 5;52(1):33-8. doi: 10.1016/j.neuron.2006.09.026.
10. George JM, Jin H, Woods WS, Clayton DF. Characterization of a novel protein regulated during the critical period for song learning in the zebra finch. Neuron. 1995 Aug;15(2):361-72. doi: 10.1016/0896-6273(95)90040-3.

11. Sode K, Ochiai S, Kobayashi N, Usuzaka E. Effect of reparation of repeat sequences in the human alpha-synuclein on fibrillation ability. Int J Biol Sci. 2006 Oct 2;3(1):1-7. doi: 10.7150/ijbs.3.1.
12. Burré J, Sharma M, Südhof TC. Cell Biology and Pathophysiology of α-Synuclein. Cold Spring Harb Perspect Med. 2018 Mar 1;8(3):a024091. doi: 10.1101/cshperspect.a024091.
13. Weinreb PH, Zhen W, Poon AW, Conway KA, Lansbury PT Jr. NACP, a protein implicated in Alzheimer's disease and learning, is natively unfolded. Biochemistry. 1996 Oct 29;35(43):13709-15. doi: 10.1021/bi961799n.
14. Kim J. Evidence that the precursor protein of non-A beta component of Alzheimer's disease amyloid (NACP) has an extended structure primarily composed of random-coil. Mol Cells. 1997 Feb 28;7(1):78-83.
15. Chandra S, Chen X, Rizo J, Jahn R, Südhof TC. A broken alpha -helix in folded alpha -Synuclein. J Biol Chem. 2003 Apr 25;278(17):15313-8. doi: 10.1074/jbc.M213128200. Epub 2003 Feb 13.
16. Bartels T, Choi JG, Selkoe DJ. α-Synuclein occurs physiologically as a helically folded tetramer that resists aggregation. Nature. 2011 Aug 14;477(7362):107-10. doi: 10.1038/nature10324.
17. Jensen MB, Bhatia VK, Jao CC, Rasmussen JE, Pedersen SL, Jensen KJ, et al. Membrane curvature sensing by amphipathic helices: a single liposome study using α-synuclein and annexin B12. J Biol Chem. 2011 Dec 9;286(49):42603-42614. doi: 10.1074/jbc.M111.271130. Epub 2011 Sep 27.
18. Middleton ER, Rhoades E. Effects of curvature and composition on α-synuclein binding to lipid vesicles. Biophys J. 2010 Oct 6;99(7):2279-88. doi: 10.1016/j.bpj.2010.07.056.
19. Bendor JT, Logan TP, Edwards RH. The function of α-synuclein. Neuron. 2013 Sep 18;79(6):1044-66. doi: 10.1016/j.neuron.2013.09.004.
20. Iwai A, Masliah E, Yoshimoto M, Ge N, Flanagan L, de Silva HA, et al. The precursor protein of non-A beta component of Alzheimer's disease amyloid is a presynaptic protein of the central nervous system. Neuron. 1995 Feb;14(2):467-75. doi: 10.1016/0896-6273(95)90302-x.
21. Jin H, Kanthasamy A, Ghosh A, Yang Y, Anantharam V, Kanthasamy AG. α-Synuclein negatively regulates protein kinase Cδ expression to suppress apoptosis in dopaminergic neurons by reducing p300 histone acetyltransferase activity. J Neurosci. 2011 Feb 9;31(6):2035-51. doi: 10.1523/JNEUROSCI.5634-10.2011.

22. Geng X, Lou H, Wang J, Li L, Swanson AL, Sun M, et al. α-Synuclein binds the K(ATP) channel at insulin-secretory granules and inhibits insulin secretion. Am J Physiol Endocrinol Metab. 2011 Feb;300(2):E276-86. doi: 10.1152/ajpendo.00262.2010. Epub 2010 Sep 21.
23. Rodriguez-Araujo G, Nakagami H, Takami Y, Katsuya T, Akasaka H, Saitoh S, et al. Low alpha-synuclein levels in the blood are associated with insulin resistance. Sci Rep. 2015 Jul 10;5:12081. doi: 10.1038/srep12081.
24. Martinez J, Moeller I, Erdjument-Bromage H, Tempst P, Lauring B. Parkinson's disease-associated alpha-synuclein is a calmodulin substrate. J Biol Chem. 2003 May 9;278(19):17379-87. doi: 10.1074/jbc.M209020200. Epub 2003 Feb 27.
25. Park SM, Jung HY, Kim TD, Park JH, Yang CH, Kim J. Distinct roles of the N-terminal-binding domain and the C-terminal-solubilizing domain of alpha-synuclein, a molecular chaperone. J Biol Chem. 2002 Aug 9;277(32):28512-20. doi: 10.1074/jbc.M111971200. Epub 2002 May 24.
26. Burré J, Sharma M, Tsetsenis T, Buchman V, Etherton MR, Südhof TC. Alpha-synuclein promotes SNARE-complex assembly in vivo and in vitro. Science. 2010 Sep 24;329(5999):1663-7. doi: 10.1126/science.1195227. Epub 2010 Aug 26.
27. Ruipérez V, Darios F, Davletov B. Alpha-synuclein, lipids and Parkinson's disease. Prog Lipid Res. 2010 Oct;49(4):420-8. doi: 10.1016/j.plipres.2010.05.004. Epub 2010 May 23.
28. Zhu M, Qin ZJ, Hu D, Munishkina LA, Fink AL. Alpha-synuclein can function as an antioxidant preventing oxidation of unsaturated lipid in vesicles. Biochemistry. 2006 Jul 4;45(26):8135-42. doi: 10.1021/bi052584t.
29. Chen RHC, Wislet-Gendebien S, Samuel F, Visanji NP, Zhang G, Marsilio D, et al. α-Synuclein membrane association is regulated by the Rab3a recycling machinery and presynaptic activity. J Biol Chem. 2013 Mar 15;288(11):7438-7449. doi: 10.1074/jbc.M112.439497. Epub 2013 Jan 23. Erratum in: J Biol Chem. 2020 Oct 9;295(41):14248.
30. Peng X, Tehranian R, Dietrich P, Stefanis L, Perez RG. Alpha-synuclein activation of protein phosphatase 2A reduces tyrosine hydroxylase phosphorylation in dopaminergic cells. J Cell Sci. 2005 Aug 1;118(Pt 15):3523-30. doi: 10.1242/jcs.02481. Epub 2005 Jul 19. Erratum in: J Cell Sci. 2005 Sep 1;118(Pt 17):4073. Peng, Xiangmin M [corrected to Peng, Xiangmin].
31. Scott D, Roy S. α-Synuclein inhibits intersynaptic vesicle mobility and maintains recycling-pool homeostasis. J Neurosci. 2012 Jul 25;32(30):10129-35. doi: 10.1523/JNEUROSCI.0535-12.2012.

32. Oueslati A, Fournier M, Lashuel HA. Role of post-translational modifications in modulating the structure, function and toxicity of alpha-synuclein: implications for Parkinson's disease pathogenesis and therapies. Prog Brain Res. 2010;183:115-45. doi: 10.1016/S0079-6123(10)83007-9.

33. Spillantini MG, Schmidt ML, Lee VM, Trojanowski JQ, Jakes R, Goedert M. Alpha-synuclein in Lewy bodies. Nature. 1997 Aug 28;388(6645):839-40. doi: 10.1038/42166.

34. Dickson DW, Ruan D, Crystal H, Mark MH, Davies P, Kress Y, et al. Hippocampal degeneration differentiates diffuse Lewy body disease (DLBD) from Alzheimer's disease: light and electron microscopic immunocytochemistry of CA2-3 neurites specific to DLBD. Neurology. 1991 Sep;41(9):1402-9. doi: 10.1212/wnl.41.9.1402.

35. Spillantini MG, Crowther RA, Jakes R, Hasegawa M, Goedert M. alpha-Synuclein in filamentous inclusions of Lewy bodies from Parkinson's disease and dementia with lewy bodies. Proc Natl Acad Sci U S A. 1998 May 26;95(11):6469-73. doi: 10.1073/pnas.95.11.6469.

36. Riccò M, Vezzosi L, Balzarini F, Gualerzi G, Ranzieri S, Signorelli C, et al. Prevalence of Parkinson Disease in Italy: a systematic review and meta-analysis. Acta Biomed. 2020 Sep 7;91(3):e2020088. doi: 10.23750/abm.v91i3.9443.

37. Hayes MT. Parkinson's Disease and Parkinsonism. Am J Med. 2019 Jul;132(7):802-807. doi: 10.1016/j.amjmed.2019.03.001. Epub 2019 Mar 16.

38. Postuma RB, Berg D, Stern M, Poewe W, Olanow CW, Oertel W, et al. MDS clinical diagnostic criteria for Parkinson's disease. Mov Disord. 2015 Oct;30(12):1591-601. doi: 10.1002/mds.26424.

39. Abbott RD, Petrovitch H, White LR, Masaki KH, Tanner CM, Curb JD, et al. Frequency of bowel movements and the future risk of Parkinson's disease. Neurology. 2001 Aug 14;57(3):456-62. doi: 10.1212/wnl.57.3.456.

40. Abbott RD, Ross GW, White LR, Sanderson WT, Burchfiel CM, Kashon M, et al. Environmental, life-style, and physical precursors of clinical Parkinson's disease: recent findings from the Honolulu-Asia Aging Study. J Neurol. 2003 Oct;250 Suppl 3:III30-9. doi: 10.1007/s00415-003-1306-7.

41. Haehner A, Boesveldt S, Berendse HW, Mackay-Sim A, Fleischmann J, Silburn PA, et al. Prevalence of smell loss in Parkinson's disease--a multicenter study. Parkinsonism Relat Disord. 2009 Aug;15(7):490-4. doi: 10.1016/j.parkreldis.2008.12.005. Epub 2009 Jan 11

42. Högl B, Stefani A, Videnovic A. Idiopathic REM sleep behaviour disorder and neurodegeneration - an update. Nat Rev Neurol. 2018 Jan;14(1):40-55. doi: 10.1038/nrneurol.2017.157. Epub 2017 Nov 24.
43. Kaufmann H, Norcliffe-Kaufmann L, Palma JA, Biaggioni I, Low PA, Singer W, et al. Natural history of pure autonomic failure: A United States prospective cohort. Ann Neurol. 2017 Feb;81(2):287-297. doi: 10.1002/ana.24877.
44. Aarsland D, Andersen K, Larsen JP, Lolk A, Kragh-Sørensen P. Prevalence and characteristics of dementia in Parkinson disease: an 8-year prospective study. Arch Neurol. 2003 Mar;60(3):387-92. doi: 10.1001/archneur.60.3.387.
45. Levy G, Schupf N, Tang MX, Cote LJ, Louis ED, Mejia H, et al. Combined effect of age and severity on the risk of dementia in Parkinson's disease. Ann Neurol. 2002 Jun;51(6):722-9. doi: 10.1002/ana.10219.
46. Hely MA, Reid WG, Adena MA, Halliday GM, Morris JG. The Sydney multicenter study of Parkinson's disease: the inevitability of dementia at 20 years. Mov Disord. 2008 Apr 30;23(6):837-44. doi: 10.1002/mds.21956.
47. Compta Y, Parkkinen L, O'Sullivan SS, Vandrovcova J, Holton JL, Collins C, et al. Lewy- and Alzheimer-type pathologies in Parkinson's disease dementia: which is more important? Brain. 2011 May;134(Pt 5):1493-1505. doi: 10.1093/brain/awr031.
48. Walker Z, Possin KL, Boeve BF, Aarsland D. Lewy body dementias. Lancet. 2015 Oct 24;386(10004):1683-97. doi: 10.1016/S0140-6736(15)00462-6.
49. Vann Jones SA, O'Brien JT. The prevalence and incidence of dementia with Lewy bodies: a systematic review of population and clinical studies. Psychol Med. 2014 Mar;44(4):673-83. doi: 10.1017/S0033291713000494. Epub 2013 Mar 25. Erratum in: Psychol Med. 2014 Mar;44(4):684.
50. Donaghy PC, Taylor JP, O'Brien JT, Barnett N, Olsen K, Colloby SJ, et al. Neuropsychiatric symptoms and cognitive profile in mild cognitive impairment with Lewy bodies. Psychol Med. 2018 Oct;48(14):2384-2390. doi: 10.1017/S0033291717003956. Epub 2018 Jan 24.
51. Ferman TJ, Smith GE, Kantarci K, Boeve BF, Pankratz VS, Dickson DW, et al. Nonamnestic mild cognitive impairment progresses to dementia with Lewy bodies. Neurology. 2013 Dec 3;81(23):2032-8. doi: 10.1212/01.wnl.0000436942.55281.47. Epub 2013 Nov 8.

52. McKeith IG, Ferman TJ, Thomas AJ, Blanc F, Boeve BF, Fujishiro H, et al. Research criteria for the diagnosis of prodromal dementia with Lewy bodies. Neurology. 2020 Apr 28;94(17):743-755. doi: 10.1212/WNL.0000000000009323. Epub 2020 Apr 2.

53. Bower JH, Maraganore DM, McDonnell SK, Rocca WA. Incidence of progressive supranuclear palsy and multiple system atrophy in Olmsted County, Minnesota, 1976 to 1990. Neurology. 1997 Nov;49(5):1284-8. doi: 10.1212/wnl.49.5.1284.

54. Gilman S, Wenning GK, Low PA, Brooks DJ, Mathias CJ, Trojanowski JQ, et al. Second consensus statement on the diagnosis of multiple system atrophy. Neurology. 2008 Aug 26;71(9):670-6. doi: 10.1212/01.wnl.0000324625.00404.15.

55. Peng C, Gathagan RJ, Lee VM. Distinct α-Synuclein strains and implications for heterogeneity among α-Synucleinopathies. Neurobiol Dis. 2018 Jan;109(Pt B):209-218. doi: 10.1016/j.nbd.2017.07.018. Epub 2017 Jul 24.

56. Woerman AL, Watts JC, Aoyagi A, Giles K, Middleton LT, Prusiner SB. α-Synuclein: Multiple System Atrophy Prions. Cold Spring Harb Perspect Med. 2018 Jul 2;8(7):a024588. doi: 10.1101/cshperspect.a024588.

57. Jecmenica-Lukic M, Poewe W, Tolosa E, Wenning GK. Premotor signs and symptoms of multiple system atrophy. Lancet Neurol. 2012 Apr;11(4):361-8. doi: 10.1016/S1474-4422(12)70022-4. Epub 2012 Mar 19.

58. Kim WS, Kågedal K, Halliday GM. Alpha-synuclein biology in Lewy body diseases. Alzheimers Res Ther. 2014 Oct 27;6(5):73. doi: 10.1186/s13195-014-0073-2.

59. Yoshida M. Multiple system atrophy: alpha-synuclein and neuronal degeneration. Neuropathology. 2007 Oct;27(5):484-93. doi: 10.1111/j.1440-1789.2007.00841.x.

60. Prusiner SB. Prions. Proc Natl Acad Sci U S A. 1998 Nov 10;95(23):13363-83. doi: 10.1073/pnas.95.23.13363.

61. Parchi P, Strammiello R, Giese A, Kretzschmar H. Phenotypic variability of sporadic human prion disease and its molecular basis: past, present, and future. Acta Neuropathol. 2011 Jan;121(1):91-112. doi: 10.1007/s00401-010-0779-6. Epub 2010 Nov 24.

62. Braak H, Del Tredici K, Rüb U, de Vos RA, Jansen Steur EN, Braak E. Staging of brain pathology related to sporadic Parkinson's disease. Neurobiol Aging. 2003 Mar-Apr;24(2):197-211. doi: 10.1016/s0197-4580(02)00065-9.

63. Kordower JH, Chu Y, Hauser RA, Freeman TB, Olanow CW. Lewy body-like pathology in long-term embryonic nigral transplants in Parkinson's disease. Nat Med. 2008 May;14(5):504-6. doi: 10.1038/nm1747. Epub 2008 Apr 6.

64. Li JY, Englund E, Holton JL, Soulet D, Hagell P, Lees AJ, et al. Lewy bodies in grafted neurons in subjects with Parkinson's disease suggest host-to-graft disease propagation. Nat Med. 2008 May;14(5):501-3. doi: 10.1038/nm1746. Epub 2008 Apr 6.

65. Desplats P, Lee HJ, Bae EJ, Patrick C, Rockenstein E, Crews L, et al. Inclusion formation and neuronal cell death through neuron-to-neuron transmission of alpha-synuclein. Proc Natl Acad Sci U S A. 2009 Aug 4;106(31):13010-5. doi: 10.1073/pnas.0903691106. Epub 2009 Jul 27. Erratum in: Proc Natl Acad Sci U S A. 2009 Oct 13;106(41):17606. PMID: 19651612; PMCID: PMC2722313.

66. Kordower JH, Dodiya HB, Kordower AM, Terpstra B, Paumier K, Madhavan L, et al. Transfer of host-derived α synuclein to grafted dopaminergic neurons in rat. Neurobiol Dis. 2011 Sep;43(3):552-7. doi: 10.1016/j.nbd.2011.05.001. Epub 2011 May 12.

67. Mougenot AL, Nicot S, Bencsik A, Morignat E, Verchère J, Lakhdar L, et al. Prion-like acceleration of a synucleinopathy in a transgenic mouse model. Neurobiol Aging. 2012 Sep;33(9):2225-8. doi: 10.1016/j.neurobiolaging.2011.06.022. Epub 2011 Aug 3.

68. Luk KC, Song C, O'Brien P, Stieber A, Branch JR, Brunden KR, et al. Exogenous alpha-synuclein fibrils seed the formation of Lewy body-like intracellular inclusions in cultured cells. Proc Natl Acad Sci U S A. 2009 Nov 24;106(47):20051-6. doi: 10.1073/pnas.0908005106. Epub 2009 Nov 5.

69. Luk KC, Kehm V, Carroll J, Zhang B, O'Brien P, Trojanowski JQ, et al. Pathological α-synuclein transmission initiates Parkinson-like neurodegeneration in nontransgenic mice. Science. 2012 Nov 16;338(6109):949-53. doi: 10.1126/science.1227157.

70. Masuda-Suzukake M, Nonaka T, Hosokawa M, Oikawa T, Arai T, Akiyama H, et al. Prion-like spreading of pathological α-synuclein in brain. Brain. 2013 Apr;136(Pt 4):1128-38. doi: 10.1093/brain/awt037. Epub 2013 Mar 6.

71. Volpicelli-Daley LA, Luk KC, Patel TP, Tanik SA, Riddle DM, Stieber A, et al. Exogenous α-synuclein fibrils induce Lewy body pathology leading to synaptic dysfunction and neuron death. Neuron. 2011 Oct 6;72(1):57-71. doi: 10.1016/j.neuron.2011.08.033.

72. Lee HJ, Patel S, Lee SJ. Intravesicular localization and exocytosis of alpha-synuclein and its aggregates. J Neurosci. 2005 Jun 22;25(25):6016-24. doi: 10.1523/JNEUROSCI.0692-05.2005.

73. Emmanouilidou E, Melachroinou K, Roumeliotis T, Garbis SD, Ntzouni M, Margaritis LH, et al. Cell-produced alpha-synuclein is secreted in a calcium-dependent manner by exosomes and impacts neuronal survival. J Neurosci. 2010 May 19;30(20):6838-51. doi: 10.1523/JNEUROSCI.5699-09.2010.

74. Jang A, Lee HJ, Suk JE, Jung JW, Kim KP, Lee SJ. Non-classical exocytosis of alpha-synuclein is sensitive to folding states and promoted under stress conditions. J Neurochem. 2010 Jun;113(5):1263-74. doi: 10.1111/j.1471-4159.2010.06695.x. Epub 2010 Mar 24.

75. Mao X, Ou MT, Karuppagounder SS, Kam TI, Yin X, Xiong Y, et al. Pathological α-synuclein transmission initiated by binding lymphocyte-activation gene 3. Science. 2016 Sep 30;353(6307):aah3374. doi: 10.1126/science.aah3374.

76. Ferreira DG, Temido-Ferreira M, Vicente Miranda H, Batalha VL, Coelho JE, Szegö ÉM, et al. α-synuclein interacts with PrP^{C} to induce cognitive impairment through mGluR5 and NMDAR2B. Nat Neurosci. 2017 Nov;20(11):1569-1579. doi: 10.1038/nn.4648. Epub 2017 Sep 25.

77. Shrivastava AN, Redeker V, Fritz N, Pieri L, Almeida LG, Spolidoro M, et al. α-synuclein assemblies sequester neuronal α3-Na+/K+-ATPase and impair Na+ gradient. EMBO J. 2015 Oct 1;34(19):2408-23. doi: 10.15252/embj.201591397. Epub 2015 Aug 31.

78. Kisos H, Pukaß K, Ben-Hur T, Richter-Landsberg C, Sharon R. Increased neuronal α-synuclein pathology associates with its accumulation in oligodendrocytes in mice modeling α-synucleinopathies. PLoS One. 2012;7(10):e46817. doi: 10.1371/journal.pone.0046817. Epub 2012 Oct 15.

79. Reyes JF, Rey NL, Bousset L, Melki R, Brundin P, Angot E. Alpha-synuclein transfers from neurons to oligodendrocytes. Glia. 2014 Mar;62(3):387-98. doi: 10.1002/glia.22611. Epub 2013 Dec 31.

80. Braak H, Rüb U, Gai WP, Del Tredici K. Idiopathic Parkinson's disease: possible routes by which vulnerable neuronal types may be subject to neuroinvasion by an unknown pathogen. J Neural Transm (Vienna). 2003 May;110(5):517-36. doi: 10.1007/s00702-002-0808-2.

81. Shannon KM, Keshavarzian A, Dodiya HB, Jakate S, Kordower JH. Is alpha-synuclein in the colon a biomarker for premotor Parkinson's disease? Evidence from 3 cases. Mov Disord. 2012 May;27(6):716-9. doi: 10.1002/mds.25020. Epub 2012 May 1. PMID: 22550057.

82. Stokholm MG, Danielsen EH, Hamilton-Dutoit SJ, Borghammer P. Pathological α-synuclein in gastrointestinal tissues from prodromal Parkinson disease patients. Ann Neurol. 2016 Jun;79(6):940-9. doi: 10.1002/ana.24648. Epub 2016 Apr 9.

83. Hilton D, Stephens M, Kirk L, Edwards P, Potter R, Zajicek J, et al. Accumulation of α-synuclein in the bowel of patients in the pre-clinical phase of Parkinson's disease. Acta Neuropathol. 2014 Feb;127(2):235-41. doi: 10.1007/s00401-013-1214-6. Epub 2013 Nov 17.

84. Breid S, Bernis ME, Babila JT, Garza MC, Wille H, Tamgüney G. Neuroinvasion of α-Synuclein Prionoids after Intraperitoneal and Intraglossal Inoculation. J Virol. 2016 Sep 29;90(20):9182-93. doi: 10.1128/JVI.01399-16.

85. Ayers JI, Brooks MM, Rutherford NJ, Howard JK, Sorrentino ZA, Riffe CJ, et al. Robust Central Nervous System Pathology in Transgenic Mice following Peripheral Injection of α-Synuclein Fibrils. J Virol. 2017 Jan 3;91(2):e02095-16. doi: 10.1128/JVI.02095-16.

86. van Keulen LJ, Vromans ME, Dolstra CH, Bossers A, van Zijderveld FG. Pathogenesis of bovine spongiform encephalopathy in sheep. Arch Virol. 2008;153(3):445-53. doi: 10.1007/s00705-007-0007-4. Epub 2007 Dec 19.

87. McBride PA, Schulz-Schaeffer WJ, Donaldson M, Bruce M, Diringer H, Kretzschmar HA, et al. Early spread of scrapie from the gastrointestinal tract to the central nervous system involves autonomic fibers of the splanchnic and vagus nerves. J Virol. 2001 Oct;75(19):9320-7. doi: 10.1128/JVI.75.19.9320-9327.2001.

88. Hoffmann C, Ziegler U, Buschmann A, Weber A, Kupfer L, Oelschlegel A, et al. Prions spread via the autonomic nervous system from the gut to the central nervous system in cattle incubating bovine spongiform encephalopathy. J Gen Virol. 2007 Mar;88(Pt 3):1048-1055. doi: 10.1099/vir.0.82186-0.

89. Parchi P, Giese A, Capellari S, Brown P, Schulz-Schaeffer W, Windl O, et al. Classification of sporadic Creutzfeldt-Jakob disease based on molecular and phenotypic analysis of 300 subjects. Ann Neurol. 1999 Aug;46(2):224-33.

90. Bartz JC. Prion Strain Diversity. Cold Spring Harb Perspect Med. 2016 Dec 1;6(12):a024349. doi: 10.1101/cshperspect.a024349.

91. Guo JL, Covell DJ, Daniels JP, Iba M, Stieber A, Zhang B, et al. Distinct α-synuclein strains differentially promote tau inclusions in neurons. Cell. 2013 Jul 3;154(1):103-17. doi: 10.1016/j.cell.2013.05.057.

92. Bousset L, Pieri L, Ruiz-Arlandis G, Gath J, Jensen PH, Habenstein B, et al. Structural and functional characterization of two alpha-synuclein strains. Nat Commun. 2013;4:2575. doi: 10.1038/ncomms3575.

93. Peelaerts W, Bousset L, Van der Perren A, Moskalyuk A, Pulizzi R, Giugliano M, et al. α-Synuclein strains cause distinct synucleinopathies after local and systemic administration. Nature. 2015 Jun 18;522(7556):340-4. doi: 10.1038/nature14547. Epub 2015 Jun 10.

94. Kim C, Lv G, Lee JS, Jung BC, Masuda-Suzukake M, Hong CS, et al. Exposure to bacterial endotoxin generates a distinct strain of α-synuclein fibril. Sci Rep. 2016 Aug 4;6:30891. doi: 10.1038/srep30891.

95. Lau A, So RWL, Lau HHC, Sang JC, Ruiz-Riquelme A, Fleck , et al. α-Synuclein strains target distinct brain regions and cell types. Nat Neurosci. 2020 Jan;23(1):21-31. doi: 10.1038/s41593-019-0541-x. Epub 2019 Dec 2.

96. Woerman AL, Stöhr J, Aoyagi A, Rampersaud R, Krejciova Z, Watts JC, et al. Propagation of prions causing synucleinopathies in cultured cells. Proc Natl Acad Sci U S A. 2015 Sep 1;112(35):E4949-58. doi: 10.1073/pnas.1513426112. Epub 2015 Aug 18.

97. Yamasaki TR, Holmes BB, Furman JL, Dhavale DD, Su BW, Song ES, et al. Parkinson's disease and multiple system atrophy have distinct α-synuclein seed characteristics. J Biol Chem. 2019 Jan 18;294(3):1045-1058. doi: 10.1074/jbc.RA118.004471. Epub 2018 Nov 26.

98. Prusiner SB, Woerman AL, Mordes DA, Watts JC, Rampersaud R, Berry DB, et al. Evidence for α-synuclein prions causing multiple system atrophy in humans with parkinsonism. Proc Natl Acad Sci U S A. 2015 Sep 22;112(38):E5308-17. doi: 10.1073/pnas.1514475112. Epub 2015 Aug 31.

99. Peng C, Gathagan RJ, Covell DJ, Medellin C, Stieber A, Robinson JL, et al. Cellular milieu imparts distinct pathological α-synuclein strains in α-synucleinopathies. Nature. 2018 May;557(7706):558-563. doi: 10.1038/s41586-018-0104-4. Epub 2018 May 9.

100. Strohäker T, Jung BC, Liou SH, Fernandez CO, Riedel D, Becker S, et al. Structural heterogeneity of α-synuclein fibrils amplified from patient brain extracts. Nat Commun. 2019 Dec 4;10(1):5535. doi: 10.1038/s41467-019-13564-w.

101. Schweighauser M, Shi Y, Tarutani A, Kametani F, Murzin AG, Ghetti B, et al. Structures of α-synuclein filaments from multiple system atrophy. Nature. 2020 Sep;585(7825):464-469. doi: 10.1038/s41586-020-2317-6. Epub 2020 May 27.

102. Prusiner SB. Novel proteinaceous infectious particles cause scrapie. Science. 1982 Apr 9;216(4542):136-44. doi: 10.1126/science.6801762. PMID: 6801762.
103. Kocisko DA, Come JH, Priola SA, Chesebro B, Raymond GJ, Lansbury PT, et al. Cell-free formation of protease-resistant prion protein. Nature. 1994 Aug 11;370(6489):471-4. doi: 10.1038/370471a0.
104. Saborio GP, Permanne B, Soto C. Sensitive detection of pathological prion protein by cyclic amplification of protein misfolding. Nature. 2001 Jun 14;411(6839):810-3. doi: 10.1038/35081095.
105. Barria MA, Mukherjee A, Gonzalez-Romero D, Morales R, Soto C. De novo generation of infectious prions in vitro produces a new disease phenotype. PLoS Pathog. 2009 May;5(5):e1000421. doi: 10.1371/journal.ppat.1000421. Epub 2009 May 15. Erratum in: PLoS Pathog. 2013 Mar;9(3). doi:10.1371/annotation/4b55946a-edb5-4feb-aeb5-2ee160394d17.
106. Colby DW, Zhang Q, Wang S, Groth D, Legname G, Riesner D, et al. Prion detection by an amyloid seeding assay. Proc Natl Acad Sci U S A. 2007 Dec 26;104(52):20914-9. doi: 10.1073/pnas.0710152105. Epub 2007 Dec 20. Erratum in: Proc Natl Acad Sci U S A. 2008 Feb 5;105(5):1774.
107. Atarashi R, Moore RA, Sim VL, Hughson AG, Dorward DW, Onwubiko HA, et al. Ultrasensitive detection of scrapie prion protein using seeded conversion of recombinant prion protein. Nat Methods. 2007 Aug;4(8):645-50. doi: 10.1038/nmeth1066. Epub 2007 Jul 22.
108. Biancalana M, Koide S. Molecular mechanism of Thioflavin-T binding to amyloid fibrils. Biochim Biophys Acta. 2010 Jul;1804(7):1405-12. doi: 10.1016/j.bbapap.2010.04.001. Epub 2010 Apr 22.
109. Wilham JM, Orrú CD, Bessen RA, Atarashi R, Sano K, Race B, et al. Rapid end-point quantitation of prion seeding activity with sensitivity comparable to bioassays. PLoS Pathog. 2010 Dec 2;6(12):e1001217. doi: 10.1371/journal.ppat.1001217.
110. Zerr I, Parchi P. Sporadic Creutzfeldt-Jakob disease. Handb Clin Neurol. 2018;153:155-174. doi: 10.1016/B978-0-444-63945-5.00009-X.
111. Ferreira NC, Charco JM, Plagenz J, Orru CD, Denkers ND, Metrick MA 2nd, et al. Detection of chronic wasting disease in mule and white-tailed deer by RT-QuIC analysis of outer ear. Sci Rep. 2021 Apr 8;11(1):7702. doi: 10.1038/s41598-021-87295-8.

112. Orrú CD, Bongianni M, Tonoli G, Ferrari S, Hughson AG, Groveman BR, et al. A test for Creutzfeldt-Jakob disease using nasal brushings. N Engl J Med. 2014 Aug 7;371(6):519-29. doi: 10.1056/NEJMoa1315200. Erratum in: N Engl J Med. 2014 Nov 6;371(19):1852.
113. Lattanzio F, Abu-Rumeileh S, Franceschini A, Kai H, Amore G, Poggiolini I, et al. Prion-specific and surrogate CSF biomarkers in Creutzfeldt-Jakob disease: diagnostic accuracy in relation to molecular subtypes and analysis of neuropathological correlates of p-tau and Aβ42 levels. Acta Neuropathol. 2017 Apr;133(4):559-578. doi: 10.1007/s00401-017-1683-0. Epub 2017 Feb 15.
114. Candelise N, Baiardi S, Franceschini A, Rossi M, Parchi P. Towards an improved early diagnosis of neurodegenerative diseases: the emerging role of in vitro conversion assays for protein amyloids. Acta Neuropathol Commun. 2020 Jul 25;8(1):117. doi: 10.1186/s40478-020-00990-x.
115. Ayers JI, Paras NA, Prusiner SB. Expanding spectrum of prion diseases. Emerg Top Life Sci. 2020 Sep 8;4(2):155-167. doi: 10.1042/ETLS20200037.
116. Simrén J, Ashton NJ, Blennow K, Zetterberg H. An update on fluid biomarkers for neurodegenerative diseases: recent success and challenges ahead. Curr Opin Neurobiol. 2020 Apr;61:29-39. doi: 10.1016/j.conb.2019.11.019. Epub 2019 Dec 13.
117. van de Beek M, van Steenoven I, van der Zande JJ, Barkhof F, Teunissen CE, van der Flier WM, et al. Prodromal Dementia With Lewy Bodies: Clinical Characterization and Predictors of Progression. Mov Disord. 2020 May;35(5):859-867. doi: 10.1002/mds.27997. Epub 2020 Feb 11.
118. van der Zande JJ, Gouw AA, van Steenoven I, van de Beek M, Scheltens P, Stam CJ, et al. Diagnostic and prognostic value of EEG in prodromal dementia with Lewy bodies. Neurology. 2020 Aug 11;95(6):e662-e670. doi: 10.1212/WNL.0000000000009977. Epub 2020 Jul 7.
119. Koga S, Aoki N, Uitti RJ, van Gerpen JA, Cheshire WP, Josephs KA, et al. When DLB, PD, and PSP masquerade as MSA: an autopsy study of 134 patients. Neurology. 2015 Aug 4;85(5):404-12. doi: 10.1212/WNL.0000000000001807. Epub 2015 Jul 2.
120. Miki Y, Foti SC, Asi YT, Tsushima E, Quinn N, Ling H, et al. Improving diagnostic accuracy of multiple system atrophy: a clinicopathological study. Brain. 2019 Sep 1;142(9):2813-2827. doi: 10.1093/brain/awz189.

121. Postuma RB, Poewe W, Litvan I, Lewis S, Lang AE, Halliday G, et al. Validation of the MDS clinical diagnostic criteria for Parkinson's disease. Mov Disord. 2018 Oct;33(10):1601-1608. doi: 10.1002/mds.27362. Epub 2018 Aug 25.
122. Koga S, Dickson DW. Recent advances in neuropathology, biomarkers and therapeutic approach of multiple system atrophy. J Neurol Neurosurg Psychiatry. 2018 Feb;89(2):175-184. doi: 10.1136/jnnp-2017-315813. Epub 2017 Aug 31.
123. Fairfoul G, McGuire LI, Pal S, Ironside JW, Neumann J, Christie S, et al. Alpha-synuclein RT-QuIC in the CSF of patients with alpha-synucleinopathies. Ann Clin Transl Neurol. 2016 Aug 28;3(10):812-818. doi: 10.1002/acn3.338.
124. Shahnawaz M, Tokuda T, Waragai M, Mendez N, Ishii R, Trenkwalder C, et al. Development of a Biochemical Diagnosis of Parkinson Disease by Detection of α-Synuclein Misfolded Aggregates in Cerebrospinal Fluid. JAMA Neurol. 2017 Feb 1;74(2):163-172. doi: 10.1001/jamaneurol.2016.4547.
125. Bongianni M, Ladogana A, Capaldi S, Klotz S, Baiardi S, Cagnin A, et al. α-Synuclein RT-QuIC assay in cerebrospinal fluid of patients with dementia with Lewy bodies. Ann Clin Transl Neurol. 2019 Oct;6(10):2120-2126. doi: 10.1002/acn3.50897. Epub 2019 Oct 10.
126. Garrido A, Fairfoul G, Tolosa ES, Martí MJ, Green A; Barcelona LRRK2 Study Group. *α*-synuclein RT-QuIC in cerebrospinal fluid of LRRK2-linked Parkinson's disease. Ann Clin Transl Neurol. 2019 May 9;6(6):1024-1032. doi: 10.1002/acn3.772.
127. Groveman BR, Orrù CD, Hughson AG, Raymond LD, Zanusso G, Ghetti B, et al. Rapid and ultra-sensitive quantitation of disease-associated α-synuclein seeds in brain and cerebrospinal fluid by αSyn RT-QuIC. Acta Neuropathol Commun. 2018 Feb 9;6(1):7. doi: 10.1186/s40478-018-0508-2. Erratum in: Acta Neuropathol Commun. 2020 Nov 5;8(1):180.
128. Shahnawaz M, Mukherjee A, Pritzkow S, Mendez N, Rabadia P, Liu X, et al. Discriminating α-synuclein strains in Parkinson's disease and multiple system atrophy. Nature. 2020 Feb;578(7794):273-277. doi: 10.1038/s41586-020-1984-7. Epub 2020 Feb 5.
129. Orrù CD, Ma TC, Hughson AG, Groveman BR, Srivastava A, Galasko D, et al. A rapid α-synuclein seed assay of Parkinson's disease CSF panel shows high diagnostic accuracy. Ann Clin Transl Neurol. 2021 Feb;8(2):374-384. doi: 10.1002/acn3.51280. Epub 2020 Dec 29.
130. Rossi M, Candelise N, Baiardi S, Capellari S, Giannini G, Orrù CD, et al. Ultrasensitive RT-QuIC assay with high sensitivity and specificity for Lewy body-associated synucleinopathies. Acta

Neuropathol. 2020 Jul;140(1):49-62. doi: 10.1007/s00401-020-02160-8. Epub 2020 Apr 27. Erratum in: Acta Neuropathol. 2020 Aug;140(2):245.

131. Rossi M, Baiardi S, Teunissen CE, Quadalti C, van de Beek M, Mammana A, et al. Diagnostic Value of the CSF α-Synuclein Real-Time Quaking-Induced Conversion Assay at the Prodromal MCI Stage of Dementia With Lewy Bodies. Neurology. 2021 Jul 1:10.1212/WNL.0000000000012438. doi: 10.1212/WNL.0000000000012438. Epub ahead of print.
132. De Luca CMG, Elia AE, Portaleone SM, Cazzaniga FA, Rossi M, Bistaffa E, et al. Efficient RT-QuIC seeding activity for α-synuclein in olfactory mucosa samples of patients with Parkinson's disease and multiple system atrophy. Transl Neurodegener. 2019 Aug 8;8:24. doi: 10.1186/s40035-019-0164-x.
133. Iranzo A, Fairfoul G, Ayudhaya ACN, Serradell M, Gelpi E, Vilaseca , et al. Detection of α-synuclein in CSF by RT-QuIC in patients with isolated rapid-eye-movement sleep behaviour disorder: a longitudinal observational study. Lancet Neurol. 2021 Mar;20(3):203-212. doi: 10.1016/S1474-4422(20)30449-X.
134. Mammana A, Baiardi S, Quadalti C, Rossi M, Donadio V, Capellari S, et al. RT-QuIC Detection of Pathological α-Synuclein in Skin Punches of Patients with Lewy Body Disease. Mov Disord. 2021 May 18. doi: 10.1002/mds.28651. Epub ahead of print.
135. Orrú CD, Groveman BR, Hughson AG, Zanusso G, Coulthart MB, Caughey B. Rapid and sensitive RT-QuIC detection of human Creutzfeldt-Jakob disease using cerebrospinal fluid. mBio. 2015 Jan 20;6(1):e02451-14. doi: 10.1128/mBio.02451-14.
136. Orrú CD, Groveman BR, Raymond LD, Hughson AG, Nonno R, Zou W, et al. Bank Vole Prion Protein As an Apparently Universal Substrate for RT-QuIC-Based Detection and Discrimination of Prion Strains. PLoS Pathog. 2015 Jun 18;11(6):e1004983. doi: 10.1371/journal.ppat.1004983. Erratum in: PLoS Pathog. 2015 Aug;11(8):e1005117.
137. Höglinger GU, Respondek G, Stamelou M, Kurz C, Josephs KA, Lang AE, et al. Clinical diagnosis of progressive supranuclear palsy: The movement disorder society criteria. Mov Disord. 2017 Jun;32(6):853-864. doi: 10.1002/mds.26987. Epub 2017 May 3.
138. Armstrong MJ, Litvan I, Lang AE, Bak TH, Bhatia KP, Borroni B, et al. Criteria for the diagnosis of corticobasal degeneration. Neurology. 2013 Jan 29;80(5):496-503. doi: 10.1212/WNL.0b013e31827f0fd1.

139. McKeith IG, Boeve BF, Dickson DW, Halliday G, Taylor JP, Weintraub D, et al. Diagnosis and management of dementia with Lewy bodies: Fourth consensus report of the DLB Consortium. Neurology. 2017 Jul 4;89(1):88-100. doi: 10.1212/WNL.0000000000004058. Epub 2017 Jun 7.
140. Dubois B, Feldman HH, Jacova C, Hampel H, Molinuevo JL, Blennow K, et al. Advancing research diagnostic criteria for Alzheimer's disease: the IWG-2 criteria. Lancet Neurol. 2014 Jun;13(6):614-29. doi: 10.1016/S1474-4422(14)70090-0. Erratum in: Lancet Neurol. 2014 Aug;13(8):757.
141. Sateia MJ. International classification of sleep disorders-third edition: highlights and modifications. Chest. 2014 Nov;146(5):1387-1394. doi: 10.1378/chest.14-0970.
142. Chandler MP, Mathias CJ. Haemodynamic responses during head-up tilt and tilt reversal in two groups with chronic autonomic failure: pure autonomic failure and multiple system atrophy. J Neurol. 2002 May;249(5):542-8. doi: 10.1007/s004150200062. PMID: 12021943.
143. Garland EM, Hooper WB, Robertson D. Pure autonomic failure. Handb Clin Neurol. 2013;117:243-57. doi: 10.1016/B978-0-444-53491-0.00020-1.
144. Albert MS, DeKosky ST, Dickson D, Dubois B, Feldman HH, Fox NC, et al. The diagnosis of mild cognitive impairment due to Alzheimer's disease: recommendations from the National Institute on Aging-Alzheimer's Association workgroups on diagnostic guidelines for Alzheimer's disease. Alzheimers Dement. 2011 May;7(3):270-9. doi: 10.1016/j.jalz.2011.03.008. Epub 2011 Apr 21.
145. van der Flier WM, Pijnenburg YA, Prins N, Lemstra AW, Bouwman FH, Teunissen CE, et al. Optimizing patient care and research: the Amsterdam Dementia Cohort. J Alzheimers Dis. 2014;41(1):313-27. doi: 10.3233/JAD-132306.
146. Fazekas F, Chawluk JB, Alavi A, Hurtig HI, Zimmerman RA. MR signal abnormalities at 1.5 T in Alzheimer's dementia and normal aging. AJR Am J Roentgenol. 1987 Aug;149(2):351-6. doi: 10.2214/ajr.149.2.351.
147. Giannini G, Calandra-Buonaura G, Asioli GM, Cecere A, Barletta G, Mignani F, et al. The natural history of idiopathic autonomic failure: The IAF-BO cohort study. Neurology. 2018 Sep 25;91(13):e1245-e1254. doi: 10.1212/WNL.0000000000006243. Epub 2018 Aug 22.
148. Frisoni GB, Boccardi M, Barkhof F, Blennow K, Cappa S, Chiotis K, et al. Strategic roadmap for an early diagnosis of Alzheimer's disease based on biomarkers. Lancet Neurol. 2017 Aug;16(8):661-676. doi: 10.1016/S1474-4422(17)30159-X. Epub 2017 Jul 11.

149. Duits FH, Teunissen CE, Bouwman FH, Visser PJ, Mattsson N, Zetterberg H, et al. The cerebrospinal fluid "Alzheimer profile": easily said, but what does it mean? Alzheimers Dement. 2014 Nov;10(6):713-723.e2. doi: 10.1016/j.jalz.2013.12.023. Epub 2014 Apr 8.
150. Slot RER, Kester MI, Van Harten AC, Jongbloed W, Bouwman FH, Teunissen CE, et al. ApoE and clusterin CSF levels influence associations between APOE genotype and changes in CSF tau, but not CSF Aβ42, levels in non-demented elderly. Neurobiol Aging. 2019 Jul;79:101-109. doi: 10.1016/j.neurobiolaging.2019.02.017. Epub 2019 Mar 1.
151. Parchi P, Strammiello R, Notari S, Giese A, Langeveld JP, Ladogana A, et al. Incidence and spectrum of sporadic Creutzfeldt-Jakob disease variants with mixed phenotype and co-occurrence of PrPSc types: an updated classification. Acta Neuropathol. 2009 Nov;118(5):659-71. doi: 10.1007/s00401-009-0585-1. Epub 2009 Aug 29. PMID: 19718500;
152. Montine TJ, Phelps CH, Beach TG, Bigio EH, Cairns NJ, Dickson DW, et al. National Institute on Aging-Alzheimer's Association guidelines for the neuropathologic assessment of Alzheimer's disease: a practical approach. Acta Neuropathol. 2012 Jan;123(1):1-11. doi: 10.1007/s00401-011-0910-3. Epub 2011 Nov 20.
153. Parchi P, de Boni L, Saverioni D, Cohen ML, Ferrer I, Gambetti P, et al. Consensus classification of human prion disease histotypes allows reliable identification of molecular subtypes: an inter-rater study among surveillance centres in Europe and USA. Acta Neuropathol. 2012 Oct;124(4):517-29. doi: 10.1007/s00401-012-1002-8. Epub 2012 Jun 30.
154. Alafuzoff I, Arzberger T, Al-Sarraj S, Bodi I, Bogdanovic N, Braak H, et al. Staging of neurofibrillary pathology in Alzheimer's disease: a study of the BrainNet Europe Consortium. Brain Pathol. 2008 Oct;18(4):484-96. doi: 10.1111/j.1750-3639.2008.00147.x. Epub 2008 Mar 26.
155. Alafuzoff I, Ince PG, Arzberger T, Al-Sarraj S, Bell J, Bodi I, et al. Staging/typing of Lewy body related alpha-synuclein pathology: a study of the BrainNet Europe Consortium. Acta Neuropathol. 2009 Jun;117(6):635-52. doi: 10.1007/s00401-009-0523-2. Epub 2009 Mar 28.
156. Baiardi S, Abu-Rumeileh S, Rossi M, Zenesini C, Bartoletti-Stella A, Polischi B, et al. CSF A*β*42/A*β*40 ratio predicts Alzheimer's disease pathology better than A*β*42 in rapidly progressive dementias. Ann Clin Transl Neurol. 2018 Dec 14;6(2):263-273. doi: 10.1002/acn3.697.
157. Willemse EAJ, van Maurik IS, Tijms BM, Bouwman FH, Franke A, Hubeek I, et al. Diagnostic performance of Elecsys immunoassays for cerebrospinal fluid Alzheimer's disease

biomarkers in a nonacademic, multicenter memory clinic cohort: The ABIDE project. Alzheimers Dement (Amst). 2018 Sep 12;10:563-572. doi: 10.1016/j.dadm.2018.08.006.

158. Abu-Rumeileh S, Steinacker P, Polischi B, Mammana A, Bartoletti-Stella A, Oeckl P, et al. CSF biomarkers of neuroinflammation in distinct forms and subtypes of neurodegenerative dementia. Alzheimers Res Ther. 2019 Dec 31;12(1):2. doi: 10.1186/s13195-019-0562-4.
159. Tijms BM, Willemse EAJ, Zwan MD, Mulder SD, Visser PJ, van Berckel BNM, et al. Unbiased Approach to Counteract Upward Drift in Cerebrospinal Fluid Amyloid-β 1-42 Analysis Results. Clin Chem. 2018 Mar;64(3):576-585. doi: 10.1373/clinchem.2017.281055. Epub 2017 Dec 5.
160. Saijo E, Groveman BR, Kraus A, Metrick M, Orrù CD, Hughson AG, et al. Ultrasensitive RT-QuIC Seed Amplification Assays for Disease-Associated Tau, α-Synuclein, and Prion Aggregates. Methods Mol Biol. 2019;1873:19-37. doi: 10.1007/978-1-4939-8820-4_2.
161. Franceschini A, Baiardi S, Hughson AG, McKenzie N, Moda F, Rossi M, et al. High diagnostic value of second generation CSF RT-QuIC across the wide spectrum of CJD prions. Sci Rep. 2017 Sep 6;7(1):10655. doi: 10.1038/s41598-017-10922-w.
162. Braune S, Reinhardt M, Schnitzer R, Riedel A, Lücking CH. Cardiac uptake of [123I]MIBG separates Parkinson's disease from multiple system atrophy. Neurology. 1999 Sep 22;53(5):1020-5. doi: 10.1212/wnl.53.5.1020.
163. Taki J, Yoshita M, Yamada M, Tonami N. Significance of 123I-MIBG scintigraphy as a pathophysiological indicator in the assessment of Parkinson's disease and related disorders: it can be a specific marker for Lewy body disease. Ann Nucl Med. 2004 Sep;18(6):453-61. doi: 10.1007/BF02984560.
164. Cramm M, Schmitz M, Karch A, Mitrova E, Kuhn F, Schroeder B, et al. Stability and Reproducibility Underscore Utility of RT-QuIC for Diagnosis of Creutzfeldt-Jakob Disease. Mol Neurobiol. 2016 Apr;53(3):1896-1904. doi: 10.1007/s12035-015-9133-2. Epub 2015 Apr 1.
165. Ruf VC, Shi S, Schmidt F, Weckbecker D, Nübling GS, Ködel U, et al. Potential sources of interference with the highly sensitive detection and quantification of alpha-synuclein seeds by qRT-QuIC. FEBS Open Bio. 2020 May;10(5):883-893. doi: 10.1002/2211-5463.12844. Epub 2020 Apr 10.
166. Saijo E, Metrick MA 2nd, Koga S, Parchi P, Litvan I, Spina S, et al. 4-Repeat tau seeds and templating subtypes as brain and CSF biomarkers of frontotemporal lobar degeneration. Acta Neuropathol. 2020 Jan;139(1):63-77. doi: 10.1007/s00401-019-02080-2. Epub 2019 Oct 16. Erratum in: Acta Neuropathol. 2019 Nov 20.

167. Kraus A, Saijo E, Metrick MA 2nd, Newell K, Sigurdson CJ, Zanusso G, et al. Seeding selectivity and ultrasensitive detection of tau aggregate conformers of Alzheimer disease. Acta Neuropathol. 2019 Apr;137(4):585-598. doi: 10.1007/s00401-018-1947-3. Epub 2018 Dec 20.
168. Scialò C, Tran TH, Salzano G, Novi G, Caponnetto C, Chiò A, et al. TDP-43 real-time quaking induced conversion reaction optimization and detection of seeding activity in CSF of amyotrophic lateral sclerosis and frontotemporal dementia patients. Brain Commun. 2020 Sep 14;2(2):fcaa142. doi: 10.1093/braincomms/fcaa142.
169. Orrú CD, Hughson AG, Groveman BR, Campbell KJ, Anson KJ, Manca M, et al. Factors That Improve RT-QuIC Detection of Prion Seeding Activity. Viruses. 2016 May 23;8(5):140. doi: 10.3390/v8050140.
170. van Rumund A, Green AJE, Fairfoul G, Esselink RAJ, Bloem BR, Verbeek MM. α-Synuclein real-time quaking-induced conversion in the cerebrospinal fluid of uncertain cases of parkinsonism. Ann Neurol. 2019 May;85(5):777-781. doi: 10.1002/ana.25447. Epub 2019 Mar 25.
171. Peden AH, McGuire LI, Appleford NEJ, Mallinson G, Wilham JM, Orrú CD, et al. Sensitive and specific detection of sporadic Creutzfeldt-Jakob disease brain prion protein using real-time quaking-induced conversion. J Gen Virol. 2012 Feb;93(Pt 2):438-449. doi: 10.1099/vir.0.033365-0. Epub 2011 Oct 26.
172. Kalia LV, Lang AE, Hazrati LN, Fujioka S, Wszolek ZK, Dickson DW, et al. Clinical correlations with Lewy body pathology in LRRK2-related Parkinson disease. JAMA Neurol. 2015 Jan;72(1):100-5. doi: 10.1001/jamaneurol.2014.2704.
173. Bloch A, Probst A, Bissig H, Adams H, Tolnay M. Alpha-synuclein pathology of the spinal and peripheral autonomic nervous system in neurologically unimpaired elderly subjects. Neuropathol Appl Neurobiol. 2006 Jun;32(3):284-95. doi: 10.1111/j.1365-2990.2006.00727.x.
174. Klos KJ, Ahlskog JE, Josephs KA, Apaydin H, Parisi JE, Boeve BF, et al. Alpha-synuclein pathology in the spinal cords of neurologically asymptomatic aged individuals. Neurology. 2006 Apr 11;66(7):1100-2. doi: 10.1212/01.wnl.0000204179.88955.fa.
175. Wakisaka Y, Furuta A, Tanizaki Y, Kiyohara Y, Iida M, Iwaki T. Age-associated prevalence and risk factors of Lewy body pathology in a general population: the Hisayama study. Acta Neuropathol. 2003 Oct;106(4):374-82. doi: 10.1007/s00401-003-0750-x. Epub 2003 Aug 2.

176. Kovacs GG, Alafuzoff I, Al-Sarraj S, Arzberger T, Bogdanovic N, Capellari S, et al. Mixed brain pathologies in dementia: the BrainNet Europe consortium experience. Dement Geriatr Cogn Disord. 2008;26(4):343-50. doi: 10.1159/000161560. Epub 2008 Oct 10.
177. Chung EJ, Babulal GM, Monsell SE, Cairns NJ, Roe CM, Morris JC. Clinical Features of Alzheimer Disease With and Without Lewy Bodies. JAMA Neurol. 2015 Jul;72(7):789-96. doi: 10.1001/jamaneurol.2015.0606.
178. DeTure MA, Dickson DW. The neuropathological diagnosis of Alzheimer's disease. Mol Neurodegener. 2019 Aug 2;14(1):32. doi: 10.1186/s13024-019-0333-5.
179. Iranzo A, Fernández-Arcos A, Tolosa E, Serradell M, Molinuevo JL, Valldeoriola F, et al. Neurodegenerative disorder risk in idiopathic REM sleep behavior disorder: study in 174 patients. PLoS One. 2014 Feb 26;9(2):e89741. doi: 10.1371/journal.pone.0089741.
180. Postuma RB, Iranzo A, Hu M, Högl B, Boeve BF, Manni R, et al.. Risk and predictors of dementia and parkinsonism in idiopathic REM sleep behaviour disorder: a multicentre study. Brain. 2019 Mar 1;142(3):744-759. doi: 10.1093/brain/awz030.
181. Stefani A, Iranzo A, Holzknecht E, Perra D, Bongianni M, Gaig C, et al. Alpha-synuclein seeds in olfactory mucosa of patients with isolated REM sleep behaviour disorder. Brain. 2021 May 7;144(4):1118-1126. doi: 10.1093/brain/awab005.
182. Fearnley JM, Lees AJ. Ageing and Parkinson's disease: substantia nigra regional selectivity. Brain. 1991 Oct;114 (Pt 5):2283-301. doi: 10.1093/brain/114.5.2283.
183. Dickson DW, Fujishiro H, DelleDonne A, Menke J, Ahmed Z, Klos KJ, et al. Evidence that incidental Lewy body disease is pre-symptomatic Parkinson's disease. Acta Neuropathol. 2008 Apr;115(4):437-44. doi: 10.1007/s00401-008-0345-7. Epub 2008 Feb 9.
184. Zetterberg H, Bendlin BB. Biomarkers for Alzheimer's disease-preparing for a new era of disease-modifying therapies. Mol Psychiatry. 2021 Jan;26(1):296-308. doi: 10.1038/s41380-020-0721-9. Epub 2020 Apr 6.
185. Cummings J. Lessons Learned from Alzheimer Disease: Clinical Trials with Negative Outcomes. Clin Transl Sci. 2018 Mar;11(2):147-152. doi: 10.1111/cts.12491. Epub 2017 Aug 2.
186. Siderowf A, Aarsland D, Mollenhauer B, Goldman JG, Ravina B. Biomarkers for cognitive impairment in Lewy body disorders: Status and relevance for clinical trials. Mov Disord. 2018 Apr;33(4):528-536. doi: 10.1002/mds.27355.